Statistical-thermodynamical analysis, using Tsallis statistics, in high energy physics

by

Andile Whitehead

Submitted to the Department of Physics
in fulfillment of the requirements for the degree of

Master of Science in Theoretical Physics

at the

UNIVERSITY OF CAPE TOWN

2014

Author .....
Department of Physics

Certified by .....
Jean Cleymans
Professor
Thesis Supervisor

Accepted by .....
Chairman
Chairman, Department Committee on Graduate Theses

Statistical-thermodynamical analysis, using Tsallis statistics, in high energy physics

by

Andile Whitehead

Submitted to the Department of Physics
in fulfillment of the
requirements for the degree of
Master of Science in Theoretical Physics

Abstract

Obatined via the maximisation of a modified entropy, the Tsallis distribution has been used to fit the transverse momentum distributions of identified particles from several high energy experiments. We propose a form of the distribution described in [1] and show it to be thermodynamically consistent. Transverse momenta distributions and fits from ALICE, ATLAS, and CMS using both Tsallis and Boltzmann distributions are presented. Tsallis fits were found to fit the p_t spectra extremely well when compared to the associated Boltzmann fits. Unfortunately universal parameters for the temperature,T, the nonextensivity parameter, q, and the fireball radius, R, could not be maintained; however, the prospect of obtaining such values, and consequently deriving relations for q and T at varying energy, $\sqrt{s}$, measured in the centre of momentum frame, appears promising.

Thesis Supervisor: Jean Cleymans
Title: Professor

Acknowledgments

Thank you to Professor Jean Cleymans and Dr. Danish Azmi without whose help this would not have been possible.

Contents

List of Figures

List of Tables

Chapter 1

Introduction

Since the advent of humanity, Man has possessed an innate curiosity. It is perhaps this nature of inquiry, that has been the primary driving force for the immense progress the human species has come to enjoy. Despite His extensive knowledge, Man still remains incapable of satisfactorily answering the essential questions posed by existentialism. Among these is that of:"Of what is nature fundamentally comprised?". The notion that all visible matter is derived from a finite set of elements was introduced by the ancient Greeks. They considered earth, water, fire and air to be the fundamental constituents of nature. However, with the development of chemistry it appeared that there were significantly more of these indivisible elements than the ancient Greeks had initially proposed. In 1869, the Russian chemist and inventor, Dmitri Mendeleev, published the periodic table of elements in which he categorised the fundamental elements of nature. For many decades scientists considered the periodic table to represent the ultimate reduction of nature into its basic constituents. However, in 1911, this view was dispelled with Rutherford's gold foil experiment in which he bombarded a strip of gold foil with alpha particles. Due to the peculiar nature with which the alpha particles were deflected from the gold strip, it was apparent that the atom could not possibly be comprised of electrons "floating" in a uniform distribution of positive charge, as suggested by the then popular plum-pudding model; instead, the atom had to possess some further internal structure with a localised positively charged nucleus surrounded by negatively charged "orbiting" electrons. It was

later discovered that the nucleus consisted of positively charged protons and neutrally charged neutrons. With this it appeared that physicists had finally succeeded in describing the principle constituents of matter. However, more remarkable findings were still on the horizon. The short-range strong force, required to bind the nucleons, inspired the Japanese physicist Hideki Yukawa to introduce the pion as the boson mediating this interaction, after which he proposed that experimentalists should look for the particle. Indeed, in 1947, the pion was found by analysing cosmic-ray radiation and with the dawn of particle accelerators, a plethora of strongly interacting subatomic particles, collectively known as hadrons, were discovered. In 1964, the quark model was postulated independently by the physicists Murray Gell-Mann and George Zweig, in order to provide an ordering scheme for the categorization of the proliferation of hadrons that were being discovered in the then high energy experiments. The model was considered purely as a method for categorizing hadrons, and not as a representation of some physical configuration within the hadrons. However,it soon became clear that the quark model was more than a tool for ordering hadrons and was in fact a physical representation of the structure of hadrons. These findings led to the establishment of the Standard Model (SM) of matter for describing the fundamental particles and force carriers in nature. Currently the SM model appears to best describe the fundamental composition of all visible matter and the interactions of these fundamental particles. Much is still unknown about the dynamical interactions of these fundamental particles and much research is still required to fully illuminate the nature of this complex subatomic world.

1.1 Quantum Chromodynamics (QCD)

1.1.1 Quarks, Gluons and Colour Charge

As described previously the quark model was independently proposed in 1964 by Gell-Mann [5] and Zweig [6] as a means to categorize the plethora of hadrons being discovered at the time. Groups, or multiplets, of baryons and mesons display a certain

orderliness in their internal quantum numbers and can be fit into geometrical patterns according to their isospin and their strangeness [7]. As a result of the quark model

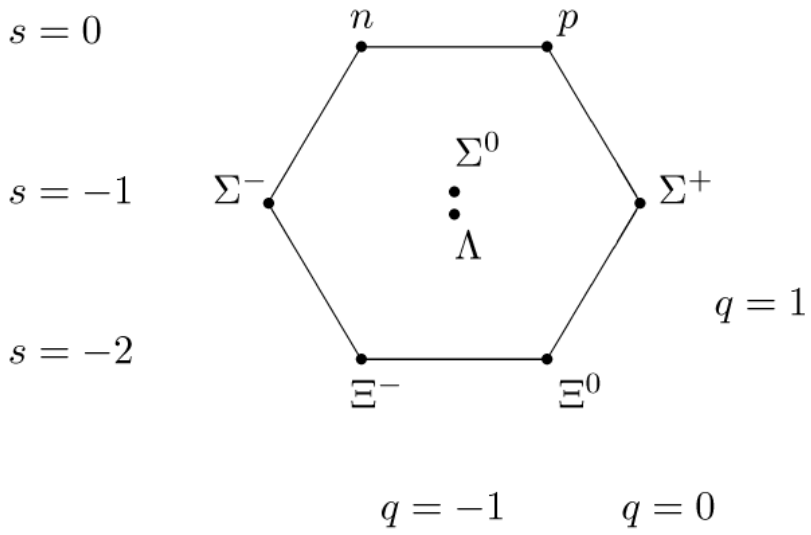

Figure 1.1: Baryon octet with $J^P = \frac{1}{2}^+$.Particles along the same horizontal line share the same strangeness number, S, those along the vertical the same isospin, I_3 , and those on the same diagonals share the same charge, Q [2]. (Image sourced from http://en.wikipedia.org/wiki/File:Baryon_octet.png)

it was realised that these geometrical arrangements of hadrons are derivative of their internal quark constituents. In the current, view the quarks are categorised into three generations, each of which contain two quarks as displayed in fig(1.2). The down (d), strange (s) and bottom (b) quarks carry an electric charge of $-\frac{1}{3}$ while the up (u), charm (c) and top (t) carry $+\frac{2}{3}$. All quarks are fermions with spin $\frac{1}{2}$ and under regular temperatures and pressures are always found in hadron bound states. These bound states can exist in one of two forms, namely, mesons or baryons. Mesons are comprised of a quark-antiquark pair ($q\bar{q}$), and baryons, consist of three quarks (qqq) or three antiquarks ($\bar{q}\bar{q}\bar{q}$). While baryons possess half integer spin and consequently obey Fermi-Dirac statistics, mesons on the other hand are integer spin hadrons and thusly adhere to Bose-Einstein statistics respectively.

It later became apparent that a further intrinsic degree of freedom had to necessarily be associated with each quark. This SU(3) (anti-symmetric) degree of freedom at-

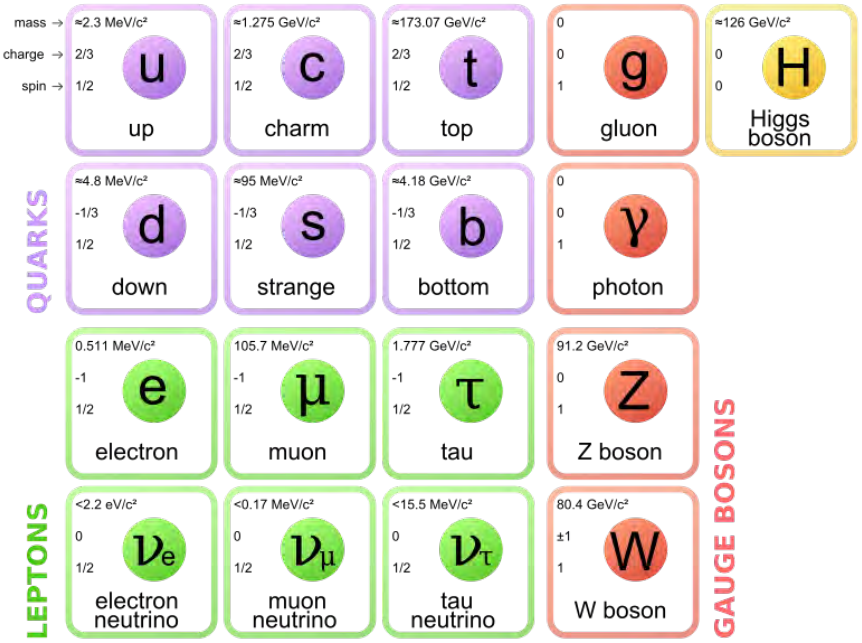

Figure 1.2: The relevant attributes of particles in the Standard Model [2]. (Image sourced from http://en.wikipedia.org/wiki/File:Standard_Model_of_Elementary_Particles.svg).

tributable to each quark, was known as colour charge. The notion of colour charge is analogous to that of electric charge; the primary difference being that three types of colour charge exist, namely, red, green, blue, along with their corresponding "negative" anti-red, anti-green and anti-blue charges appropriately associated with the antiquarks. By virtue of the fact that hadrons possessing a non-zero colour charge have not been observed in nature, the natural conclusion would thus be that the strong force must act in such a way as to ensure that the bounded quarks (along with the gluons) within the hadron exist as a combined colourless SU(3) singlet state. A combination of red, green and blue, or anti-red, anti-green and anti-blue quarks forms a colourless baryon state while an oppositely colour-charged quark-antiquark pair (e.g. red and anti-red) forms a colourless meson state.

1.1.2 The Strong Potential and Colour Confinement

The strong interaction is mediated by the set of eight gluons (forming a colour octet) that couple to colour charge [1]. The strong potential, V_s , between two opposite colour charges, can be modelled by [7]:

$$V_s = -\frac{4}{3}\frac{\alpha_s}{r} + kr \tag{1.1}$$

where r is the distance between the charges, α_s is the coupling constant of the strong interaction and k is the string tension, a factor representing the strength of the quark binding force. At short distances the first term in (1.1) dominates the behaviour of the potential, diminishing like $\sim \frac{1}{r}$ with increasing distance similar to the Coulomb potential. Perhaps somewhat less intuitively: as the distance, r, between the charges increases, the second term in (1.1) dominates V_s and gives rise to the linear behaviour of the potential at large r. This has the implication that an infinite amount of energy is required to free a quark. It is this particular property of the strong interaction, appropriately termed confinement, that explains why free quarks or colour-charged hadronic states have never been observed.

In QCD, the colour-confining nature of the strong interaction is attributable to the fact that gluons carry colour charge; consequently, unlike the electrically neutral photons, they are able to couple to one another. When the separation between two quarks exceeds $\sim 1\,\text{fm}$, the gluon-gluon coupling begins pulling the colour field lines together into string-like objects. At large enough distances it becomes more energetically favourable to create a quark-antiquark pair from the vacuum rather than further extending the length of the string.

[1] The ninth gluon forms a colourless singlet state and so does not participate in the strong interaction

1.1.3 Asymptotic Freedom

The strong coupling constant α_s in (1.1), derived in Quantum Field Theory (QFT), essentially, was determined in order to quantify the strength of the strong interaction. Deceptively, α_s is not in fact a constant at all, but rather a function of the separation between the charges, r, or the four-momentum exchange, q^2. Evidently, high momentum transfers are associated with short range interactions and vice versa and so the dependence of α_s on q^2 necessarily implies the dependence of α_s on r. The variability of the strong coupling constant, is referred to as the running coupling strength; the underlying cause for which (amongst other things) lies in the quantum fluctuations of the vacuum. Uncertainty Principle. Analogous to vacuum polarisation in QED, a colour charge can polarise the surrounding virtual quark-antiquark pairs that are created (and annihilated) by the vacuum. As a result, the polarised vacuum partially screens the colour charge, and thus reduces the magnitude of its field. However, in addition to the vacuum polarisation generated by the virtual quark pairs, an additional effect is observed: Gluons are able to couple to the exchange gluons associated with the virtual quark pairs and ultimately form a cloud of self-interacting gluons around the virtual quarks which has the peculiar effect of producing a conflicting, anti-screening effect.

Using the renormalisation technique, the strong coupling constant $\alpha_s(|q^2|)$ at a given momentum transfer, q^2 , can be expressed in terms of a measured $\alpha_s(|q_0^2|)$ at a particular $q^2 = q_0^2$. The relation describing the dependence, or "running", of the strong coupling constant with respect to q^2, as derived from QCD, is [7]:

$$\alpha_s(|q^2|) = \frac{12\pi}{\beta \ln\left(|q^2|/\Lambda^2\right)} \tag{1.2}$$

where Λ is the QCD scale constant, a parameter determined experimentally via measuring α_s at different q^2 values. Typically quoted values of Λ are of the order of $\sim 200\,\mathrm{MeV}$. The counteracting effects of the quark and gluon polarisation in creating an overall screening or anti-screening effect is controlled by the β term in (1.2). The

simple formula describing β is:

$$\beta = 11n - 2f, \tag{1.3}$$

where f and n are respectively, the postulated number of quark flavours and colour charges that occur in nature. In the theory, if $11n > 2f$ then the anti-screening effect due to the gluon-gluon coupling will dominate the screening effect of the virtual quark pairs and the effective coupling will decrease with increasing q^2. Given that there are six quark flavours and three colour charges in the theory ($\beta = -21$) this will evidently be the case. Due to the inverse correlation between r and q^2, we can equivalently state that, at short distances, the strong force effectively becomes relatively weak. This characteristic of the strong interaction is termed asymptotic freedom. The phenomenon of asymptotic freedom provides a regime in which analytical calculations for experimental observables can be performed: In the regime of high momentum transfer, where $q^2 >> \Lambda^2$, the coupling constant tends to zero. This fortuitous property of the coupling constant allows for the use of perturbation theory in QCD, [8], to make experimentally verifiable predictions, for relevant observables.

1.1.4 Quark Gluon Plasma (QGP)

Phases of Strongly Interacting Matter

Naturally, the discovery of asymptotic freedom led to speculation of a possible phase transition from partons existing within bound states of hadronic matter to a deconfined state of partons, the quark gluon plasma (QGP) [9]. Evidently, two interacting quarks situated within close proximity of one another (alternatively, large q^2), can be in a temporary state of asymptotic freedom. However, the existence of a QGP, necessitates the existence of a medium of quarks and gluons where individual partons are able, uninhibitedly, to traverse distances larger than the typical size of hadronic states. Evidently, (1.1) does not include the effects of the medium, i.e. the plasma, on the potential between the two opposite colour charges. It is this presence of numerous mobile colour charges in the QGP, that results in the screening of individual long

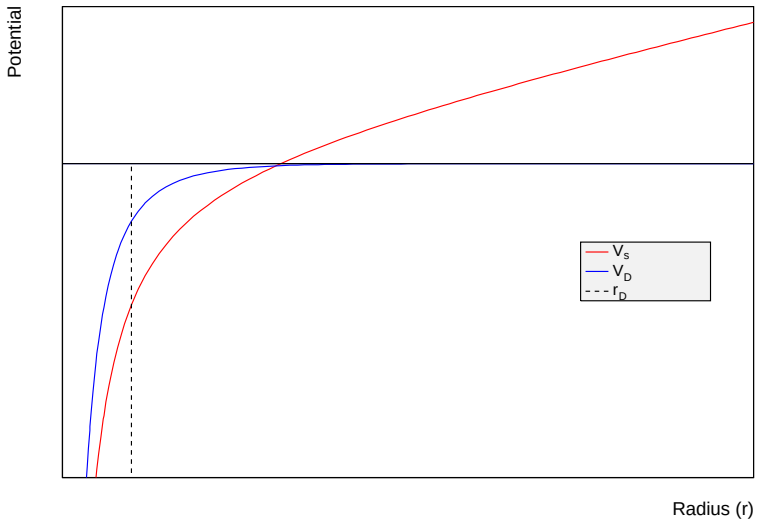

Figure 1.3: Graphic displaying the difference between the strong potential, V_s between individual quarks and the modified strong potential, V_D due to the Debye screening of the partonic medium. The dashed line represents the Debye length, r_D of the medium.

range interactions, known as Debye screening. Considering only the short range term of the QCD potential (first term in (1.1)), the presence of Debye screening modifies the potential such that:

$$V_s(T, r) \sim -\frac{\alpha_s}{r} e^{-\frac{r}{r_D}} \tag{1.4}$$

where T is the temperature of the plasma and $r_D(T)$ is the temperature dependent Debye length, which characterises the length from which the potential is screened[2]. When r_D becomes smaller than the typical radius of a hadron the strong force no longer confines the partons and the bound state dissolves. Thus, in addition to the attenuation of the coupling constant with decreasing r, increasing the density of colour charges has the effect of screening the long range influence of the strong potential. The increased density can be achieved via thermal excitation or extreme compression of a hadronic system. Consequently, the formation of a highly dense system in combination with a small coupling constant are the conditions necessary

[2]refer to fig(1.3)

for the occurrence of the phase transition from a state of hadronic matter to that of the QGP. Non-perturbative methods, such as Lattice QCD, have been used to gauge the critical temperature, T_C, and energy density, ϵ_C, at which such phase transitions occur. These calculations estimate T_C to be in the range $155-160\,\mathrm{MeV}$ and $\epsilon_C \sim 1\,\mathrm{GeV/fm}^3$ [10]. The relation between the energy density and the temperature, derived from the Stefan-Boltzmann (SB) law for the case of low net baryon density ($\mu_B \sim 0$), is [11]:

$$\frac{\epsilon}{T^4} = \left[2(n_c^2 - 1) + 2n_c n_f \frac{7}{4}\right] \frac{\pi^2}{30} \tag{1.5}$$

where n_f and n_c are the respective number of quark flavours and colour charges. The fact that the energy density lies below the SB limit indicates that quarks still undergo interactions and asymptotic freedom is not achieved, at least for $T < 4T_C$. In the QGP, quarks become deconfined and their mass drops down from the dynamical value within a hadron, of the order of $\sim 300\,\mathrm{MeV}$ (for u and d quarks), to the bare value of $\sim$ 5MeV.

Fig(1.4) shows a sketch of the phase diagram of strongly interacting matter in (μ_B, T)

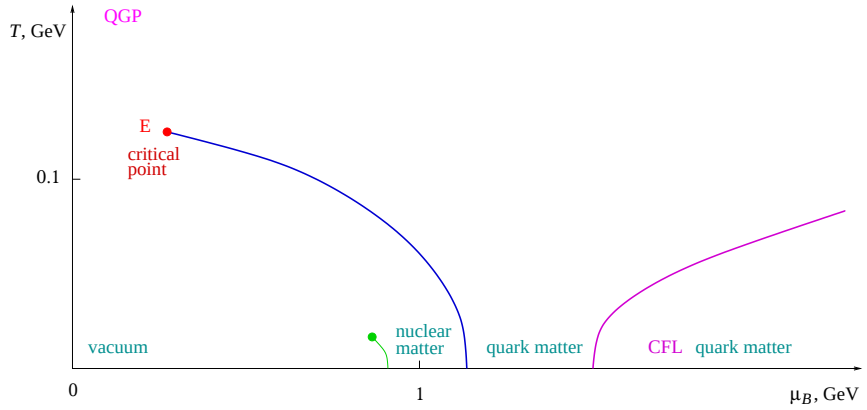

Figure 1.4: QCD phase diagram for strongly interacting matter [3]

parameter space, where the baryon chemical potential, μ_B , is essentially a measure of the asymmetry between quarks and antiquarks in the system. "Cold" nuclear matter, such as typical nuclei, occur at low T and $\mu_B \sim 900\,\mathrm{MeV}$. When excited thermally, nuclei eventually separate into protons and neutrons. During the separation, light

hadrons, primarily pions, are produced and begin to occupy the space between the nucleons. When the hadron gas that has formed is sufficiently heated or compressed, the medium attains a density sufficiently large for the effects of Debye screening to be experienced within regions of the hadron gas. Consequently, in and amongst the hadronic matter, regions of free partons form, which at the critical temperature, T_C, spreads throughout the entire volume of the hadron gas. The phase boundary with the QGP state is represented by the solid line in fig(1.4). If matter is only compressed, increasing μ_B while keeping the temperature of the system relatively low, the phase transition is located on the right side of the diagram. Based on different models the two phases are separated by a line of constant energy density across which the transition is of first order. However, according to Lattice QCD calculations, a certain critical point is reached as $\mu_B \to 0$, beyond which the transition is expected to become a rapid crossover. This is the region which is experimentally accessible in heavy-ion collisions at the SPS, RHIC and LHC, going to lower and lower μ_B as the centre-of-mass energy of the collisions increases. At $\mu_B \sim 0$, along the line where the early universe evolved, the transition is predicted to happen at a critical temperature of $T_C \approx 160\,\mathrm{MeV}$.

Ultra-relativistic heavy-ion collisions are used to probe the low μ_B and high T region of the QCD phase diagram where matter is predicted to exist in the QGP phase. The QGP formation is not observed directly, but by studying the final state of the interactions, looking for particular signatures which are expected only in systems where the QGP is produced, such as central A-A (i.e. nucleus-nucleus) collisions, and are less likely to occur in others such as p-p (proton-proton) or peripheral A-A. For this reason analyses are usually done on both A-A and p-p data in order to establish if a particular observable is due to the QGP formation (or compare A-A with different collision centralities).

1.2 Statistical Thermodynamic Models

Due to the running nature of the strong coupling constant, α_s, QCD is only perturbative within certain energy regimes, specifically, large q^2; however, in the low energy regime, due to the magnitude of α_s, the perturbative methods of QCD are inapplicable. Thus, describing low energy phenomena in QCD has necessitated the development of phenomenological models, of which there are numerous. Amongst these, thermal models are widely used and have proven to be extremely successful in reproducing experimental results for various quantities measured in heavy-ion collisions [12], [4]. Essentially, the simplest statistical-thermal models, are those that model the hadrons produced during the heavy-ion collision as a gas of non-interacting particles. When one uses such statistical models an important assumption is that the system being treated reaches equilibrium i.e. equilibrium distributions are assumed. It is extremely peculiar that such models should perform so well given that the system at chemical freeze-out (cessation of inelastic collisions) has insufficient time to equilibrate through rescattering (kinetic thermalisation); yet somehow the results obtained for the hadron yields using such models are consistent with those obtained experimentally. This raises theoretical questions about the possible statistical nature of the hadronization process.

Chapter 2

Boltzmann-Gibbs Statistics

In this section we shall briefly describe the formulation of typical statistical mechanics used in the, non-interacting hadron gas, models used to describe the particles generated in heavy-ion collisions.

When two heavy-ions collide they produce what is known as a fireball. In the primordial fireball numerous hadrons are created. In such high energy interactions, particle numbers are not conserved. However, it is known that such interactions do conserve the initial quantum number content of the interaction. This argument, distinctly ignores weak interactions. This is quite a valid assumption, since the relevant time scales are usually considerably shorter than the typical times scales for weak interactions which are typically between 11-15 orders of magnitude longer than strong interactions. Thus, when modelling the system statistically; instead of conserving particle numbers - as one would typically do - it is the initial quantum number content of the system that is conserved. However, in practice, this is not as trivial as one may assume [4]. The degree of stopping of the colliding nuclei, is evidently dependent on the beam energy, and this clearly affects the choice of baryon number and charge. Furthermore, the centrality of the collision also affects the quantum number content. The quantum numbers usually conserved when performing these calculations are baryon number, B, charge, Q, and strangeness, S and occasionally charm, C. Topness, T, and bottomness b are usually not included as it is reasonable to assume that such heavy quarks are very rarely produced (at these energies). Thus the chemical po-

tential associated with a particular hadron species, i, in the hadron gas at freeze-out is given by $\mu_i = \mu_b B_i + \mu_Q Q_i + \mu_S S_i + \mu_C C_i$, where μ_B, μ_Q, μ_S, μ_C are, respectively, the chemical potentials associated with baryon number, charge, strangeness, and charm of the system. Evidently, the net quantum number content of the system is given by:

$$B = \sum_i B_i N_i \qquad 0 = \sum_i S_i N_i \qquad Q = \sum_i Q_i N_i$$
$$0 = \sum_i C_i N_i, \tag{2.1}$$

where N_i is the number of particles of specie i in the hadron gas, and the sum in (3.1) is taken over both particles and anti-particles.

When implementing a statistical-thermal analysis of a chosen system it is necessary that one decides in which ensemble to operate [13], the choice of which largely depends on one's desired treatment of the conservation laws. There are three statistical ensembles, namely, the micro-canonical (MCE), canonical (CE) and grand canonical (GCE) ensembles that are used extensively. Of these, the MCE is the most restrictive, in that the energy and the quantum numbers in such ensembles are fixed precisely. Somewhat less restrictive is the CE in which relevant quantum numbers remain fixed but the energy; however, is set on average by the temperature, T, of the system. That is to say; if one were to measure the total energy of the system numerous times, these calculated energies would fluctuate around the average energy of the system (determined by the temperature). In the GCE, both the energy and quantum numbers, respectively, are set on average by the temperature, T, and the chemical potential/s μ_i, where i represents some conserved quantum number. With the appropriate choice of ensemble, one's task is to compute the partition function of the system under consideration. Once evaluated, the partition function can be utilised to calculate the relevant thermodynamic quantities characteristic of the fireball at freeze-out.

Generally, in the GCE, the partition function is derived via considering the transfer of energy and particles between a system and a large reservoir. We can obtain the same probability distribution function via the extremization of the Shannon-Gibbs

entropy [14] given by:

$$S = -\sum_{i}^{W} p_i \ln p_i, \tag{2.2}$$

where the index i labels each unique configuration (microstate) of the system and $W \in \mathbb{N}$ represents the total number of possible configurations of the system, with the constraints,

$$f(\{p_i\}) = \sum_{i}^{W} p_i = 1, \tag{2.3}$$

$$g(\{p_i\}) = \sum_{i}^{W} E_i p_i = \bar{E}, \tag{2.4}$$

$$h(\{p_i\}) = \sum_{i}^{W} N_i p_i = \bar{N}. \tag{2.5}$$

From information theory, entropy is a measure of our knowledge of the state of a system, where $S_1 = 0$ describes perfect knowledge of the state of the system. Thus given the constraints in (2.3-2.5) we seek to maximize the entropy, i.e. make the least biased estimate of our system given the limited information provided. When maximising a multivariable functional subject to a given number of constraints, the approach used is that of the method of Lagrange multipliers. Consequently, the variational problem that requires solving is:

$$\delta \left[S(\{p_i\}) - \alpha \delta f(\{p_i\}) - \beta \delta g(\{p_i\}) - \gamma \delta h(\{p_i\}) \right] = 0, \tag{2.6}$$

where $\alpha, \beta, \gamma \in \mathbb{R}$. Evidently (2.6) is merely a compact form of expressing W equations of the form:

$$\ln p_n + 1 = -\alpha - \beta E_n - \gamma N_n \tag{2.7}$$

where $\{n \in \mathbb{N} | n \in [1, W]\}$. (2.7) simplifies to the following expression for the probabilities of the various states of the system at equilibrium:

$$p_n = Ae^{-(\beta E_n + \gamma N_n)}, \tag{2.8}$$

where [1] $A = \exp\{-\alpha - 1\}$. Moreover, the constraint expressed in (2.3) allows for the reformulation of A into the following :

$$A = \left(\sum_i e^{-(\beta E_i + \gamma N_i)} \right)^{-1}. \tag{2.9}$$

Describing the system in terms of its possible macrostates (as opposed to microstates), (2.9) can be reformulated into the more familiar form:

$$\begin{aligned} A &= \left(\sum_{N=0}^{\infty} \sum_i e^{-(\beta E_i + \gamma N)} \right)^{-1}, \\ &= \frac{1}{Z_{GC}}, \end{aligned} \tag{2.10}$$

where the index i now represents the macrostate (defined solely by the energy and not the number of particles of the system) with energy E_i, and N the number of particles (which is run over for each particular macrostate). Hence, we can identify $A = 1/Z_{GC}$ where Z_{GC} is the partition function of GCE by identifying the parameters $\beta = \frac{1}{T}$ and $\gamma = \beta\mu$. Evidently, we have derived the probability distribution function for the GCE at equilibrium via the extremization of the SG entropy under the constraints expressed in (2.3)-(2.5), under purely statistical, non-physical, arguments.

[1] Evidently, this is under the assumption that a configuration is uniquely determined by its energy and number of particles. If not, the degeneracy of the state must be included.

2.1 Quantum Statistics

If the given system is quantum mechanical, then it will be composed of α energy levels ϵ_ν each with a given number of particles n_ν, such that $\sum n_\nu \epsilon_\nu = E_n$ and $\sum n_\nu = N$. Using this new prescription, the GC partition function is given by:

$$Z_{GC} = \sum_{N}^{\infty} \sum_{\{n_\nu\}}^{*} \prod_{\nu} e^{-\beta(\epsilon_\nu n_\nu - \mu n_\nu)} \tag{2.11}$$

$$= \sum_{\{n_\nu\}} \prod_{\nu} e^{-\beta(\epsilon_\nu n_\nu - \mu n_\nu)} \tag{2.12}$$

where $\sum_{\{n_\nu\}} = \sum_{n_1} \sum_{n_2} \dots \sum_{n_\alpha}$ and the asterisk in (2.11) is representative of the constraint: $\sum n_\nu = N$. Consequently, one can then rewrite (2.12) as:

$$Z_{GC} = \sum_{\{n_\nu\}} \prod_{\nu} \left[e^{-\beta(\epsilon_\nu - \mu)}\right]^{n_\nu} \tag{2.13}$$

$$Z_{GC} = \prod_{\nu} z_\nu, \tag{2.14}$$

where z_ν is the partition function for the ν^{th} energy level. If the system is composed of fermions then $\{n_\nu \in \mathbb{N}_0 | n \in [0,1]\}$. Resultantly:

$$z_\nu^{FD} = 1 + e^{-\beta(\epsilon_\nu - \mu)}. \tag{2.15}$$

If, instead, the system is comprised of bosons, the partition function for energy level ν is given by:

$$z_\nu^{BE} = \sum_{n_\nu=0}^{\infty} \left(e^{-\beta(\epsilon_\nu - \mu)}\right)^{n_\nu}, \tag{2.16}$$

$$= \frac{1}{1 - e^{-\beta(\epsilon_\nu - \mu)}}. \tag{2.17}$$

The average population number of a given quantum state will be given by:

$$\langle n_\nu \rangle = \frac{\sum_{n_\nu=0}^{\infty} n_\nu e^{-\beta(\epsilon_\nu n_\nu - \mu n_\nu)}}{\sum_{n_\nu=0}^{\infty} e^{-\beta(\epsilon_\nu n_\nu - \mu n_\nu)}}, \tag{2.18}$$

$$= -\frac{1}{\beta}\frac{\partial \ln z_\nu}{\partial \epsilon_\nu}, \tag{2.19}$$

which in the case of fermions and bosons is given by:

$$\langle n_\nu \rangle^{FD,BE} = \frac{1}{e^{\beta(\epsilon_\nu - \mu)} \pm 1}, \tag{2.20}$$

where the plus and minus signs denote the average occupation number for fermions and bosons respectively.

Since the average number of particles is given by:

$$\begin{aligned} N &= -\frac{\partial \Omega}{\partial \mu} \\ &= T\frac{\partial \ln Z^{GC}}{\partial \mu} \\ &= \pm T\frac{\partial \sum_\nu \ln\left(1 \pm e^{-\beta(\epsilon_\nu - \mu)}\right)}{\partial \mu} \\ &= \sum_\nu \frac{e^{-\beta(\epsilon_\nu - \mu)}}{1 \pm e^{-\beta(\epsilon_\nu - \mu)}} \\ &= \sum_\nu \langle n_\nu \rangle \end{aligned} \tag{2.21}$$

We can now multiply and divide by a factor of Δp_i, but since $\Delta p_i = 2\pi/L_i$(quantum mechanical particle in a box with continuous boundary conditions) where $i = x, y, z$ we can rewrite (2.21) as

$$\bar{N} = \sum_\nu \frac{V}{(2\pi)^3} \langle n_\nu \rangle (\Delta p_x)(\Delta p_y)(\Delta p_z) \tag{2.22}$$

where $V = \prod_i L_i$. Taking the limit where $L_i \to \infty$(the large volume approximation) we find that the average number of particles is given by:

$$\begin{aligned} \bar{N} &= V \int \frac{d^3p}{(2\pi)^3} \langle n \rangle_p \,, \\ &= V \int \frac{d^3p}{(2\pi)^3} \frac{1}{e^{\beta(\epsilon-\mu)} \pm 1}. \end{aligned} \tag{2.23}$$

Using the above result, it can be easily shown that the entropy for a gas of identical fermions/bosons is given by [2]:

$$S^{FD,BE} = -\sum_\nu \left[n_\nu \ln n_\nu \pm (1 \mp n_\nu) \ln (1 \mp n_\nu) \right]. \tag{2.24}$$

Evidently[3], in the Boltzmann limit, i.e. an ideal gas of extremely low concentration or high temperature, the expression for the average occupation number expressed in (2.20) reduces to:

$$\langle n_\nu \rangle^B = e^{-\beta(\epsilon_\nu - \mu)}. \tag{2.25}$$

Thus, using the expression for the Boltzmann approximation for the mean occupation number in (2.21), the expression for the entropy in (2.24), in the Boltzmann limit, simplifies to:

$$S^B = -\sum_\nu \left[n_\nu \ln n_\nu - n_\nu \right]. \tag{2.26}$$

One can show naturally in an analogous manner to the previous analysis that the maximization of this particular entropy with respect to the constraints:

$$g = \sum_\nu n_\nu \epsilon_\nu = \bar{E}, \tag{2.27}$$

$$h = \sum_\nu n_\nu = \bar{N}, \tag{2.28}$$

[2]This is shown in appendix A.

[3]The notation n_ν will be used in place of $< n_\nu >$ for majority of the text.

reproduces the expression for the approximated average occupation number in (2.21), and so ensuring a sort of self-consistency of the approach.

Chapter 3

Tsallis Distribution

Boltzmann-Gibbs (BG) statistics is based on the fact that the particles within a system interact over extremely small length scales, i.e. the interactions are purely the collisional interactions. Such characteristic short range interactions allows us to view the fluid as non-interacting and in turn we generate the familiar results of statistical mechanics. It is currently well established that there are numerous physical systems under which BG statistics encounters many difficulties. Some of these physical systems which include situations characterized by long-range interactions, long-range microscopic memories, and those involving a space-time (and phase space) exhibiting a (multi)fractal structure are discussed in [15],[16] and [17]. In particular, when analysing the transverse momentum (p_t) spectra of hadrons it is found that spectra decrease far slower than predicted by BG statistics, and appear to follow some power-law at high p_t . Such departures from the BG exponential are argued as being attributable to dynamical effects. Essentially, these effects survive the equilibration process and can show up as apparent departures from the assumed thermal equilibrium in the form of the enhancement of the exponential tail into power-law tail. Typically, when such observations are made, one assumes that the statistical model is too simplistic and accounts for the departure via including some additional (non-equilibrium) dynamical considerations. The most common consideration is treating the fireball as an expanding fluid, in which case the invariant momentum spectrum

is given by the Cooper-Frye formula[18]:

$$E\frac{dN}{dp^3} = \frac{g}{(2\pi)^3}\int_\sigma f(x,p)p^\mu d\sigma_\mu, \tag{3.1}$$

where $f(x,p)$ describes the distribution function $f(x,p) = \exp[(-p.u+\mu)/T]$, p and u are the 4-momentum and 4-velocity respectively and the integration is taken over the freeze-out surface σ_μ. For a static fireball, the freeze-out surface is given by $d\sigma^\mu = (dx^3, 0)$, in which case one recovers the familiar BG expression,

$$E\frac{dN}{dp^3} = \frac{gV}{(2\pi)^3}Ee^{-\frac{(E-\mu)}{T}}. \tag{3.2}$$

However, at times it can be extremely difficult to decide which dynamical remedy is appropriate and given that we have decided which dynamical phenomena are responsible for the departure from our simplistic statistical considerations, then how influential are the various dynamics to the observed spectra? Instead, one can bypass the process of such involved considerations and modify the form of the statistical model to account for these observed departures without having to actually consider the dynamics responsible for them. In an attempt to overcome at least some of the difficulties experienced due to the short comings of BG statisitics, a generalized form of the entropy was postulated in [19]. The form of the entropy is given by:

$$S_q \equiv \frac{1-\sum_{i=1}^{W} p_i^q}{q-1} \qquad q \in \mathbb{R}, \tag{3.3}$$

where q is some parameter. It can be easily shown that this newly postulated entropy is nonextensive. If we have two independent systems A and B, described by the proposed entropy in (3.3), i.e.:

$$S_q(A) = \frac{\left(1-\sum_i p_{A,i}^q\right)}{q-1}, \tag{3.4}$$

$$S_q(B) = \frac{\left(1-\sum_i p_{B,i}^q\right)}{q-1}, \tag{3.5}$$

then the entropy of the combined system is given by:

$$\begin{aligned}
S_q(A+B) &= \frac{\left(1-\sum_k p_{AB,k}^q\right)}{q-1}, \\
&= \frac{\left(1-\sum_i\sum_j p_{A,i}^q p_{B,j}^q\right)}{q-1}, \\
&= \frac{2-\sum_i p_{A,i}^q - \sum_j p_{B,j}^q - \left(1-\sum_i p_{A,i}^q\right)\left(1-\sum_j p_{B,j}^q\right)}{q-1}, \\
&= \frac{\left(1-\sum_i p_{A,i}^q\right)}{q-1} + \frac{\left(1-\sum_j p_{B,j}^q\right)}{q-1} - (q-1)\frac{\left(1-\sum_i p_{A,i}^q\right)}{q-1}\frac{\left(1-\sum_j p_{B,j}^q\right)}{q-1}, \\
&= S_q(A) + S_q(B) + (1-q)S_q(A)S_q(B). \qquad (3.6)
\end{aligned}$$

Evidently the third term in (3.6) makes the entropy nonextensive. Furthermore, if we allow for $q \to 1$, we have:

$$\begin{aligned}
S_1 &\equiv \lim_{q\to 1} S_q, \\
&= \lim_{q\to 1} k\frac{1-\sum_{i=1}^W p_i p_i^{q-1}}{q-1}, \\
&= \lim_{q\to 1} k\frac{1-\sum_{i=1}^W p_i \exp\{(q-1)\ln(p_i)\}}{q-1}. \qquad (3.7)
\end{aligned}$$

We can then perform a Taylor expansion of the exponential term in (3.7) about $q = 1$ to give,

$$S_1 = \lim_{q\to 1} \frac{1-\sum_{i=1}^W p_i\left[1+(q-1)\ln p_i + \frac{(q-1)^2(\ln p_i)^2}{2!} + \frac{(q-1)^3(\ln p_i)^3}{3!} + \ldots\right]}{q-1}, \qquad (3.8)$$

and using the fact that $\sum_{i=1}^W p_i = 1$, (3.8) becomes:

$$\begin{aligned}
S_1 &= \lim_{q\to 1}\left[-\sum_{i=1}^W p_i\ln p_i - \sum_{i=1}^W p_i\frac{(q-1)(\ln p_i)^2}{2!} - \sum_{i=1}^W p_i\frac{(q-1)^2(\ln p_i)^3}{3!} + \ldots\right], \\
&= -\sum_{i=1}^W p_i\ln p_i. \qquad (3.9)
\end{aligned}$$

Evidently from (3.9), it is apparent that as $q \to 1$ the generalised nonextensive Tsallis entropy tends towards the familiar extensive Shannon-Gibbs entropy. It is clear from this that q is some measure of the nonextensivity of the entropy of the system. Unfortunately, it does not reveal the cause of this departure from the standard Shanon-Gibbs entropy. This must be deduced from the system.

Using the entropy expressed in (2.2), we can reformulate the different distributions, at equilibrium, characterised by the different ensembles within the framework of Tsallis statistics. In a similar vain to that of BG statistics we maximise the Tsallis entropy subject to the constraints associated with the particular ensemble of interest.

3.1 Micro-Canonical Ensemble

The micro-canonical ensemble has one constraint; namely,

$$\begin{aligned} f &= \sum_{i=1}^{W} p_i, \\ &= 1. \end{aligned} \tag{3.10}$$

The method of Lagrange multipliers gives the variational equation:

$$\delta \left[S(\{p_i\}) - \alpha f \right] = 0. \tag{3.11}$$

This gives W equations of the form:

$$\begin{aligned} \frac{q p_n^{q-1}}{q-1} &= \alpha \\ p_n &= \left(\frac{q-1}{q} \right)^{\frac{1}{q-1}} \alpha^{\frac{1}{q-1}}. \end{aligned} \tag{3.12}$$

Using the constraint in (3.10), we acquire the condition that

$$\alpha^{\frac{1}{q-1}} = \frac{1}{W} \left(\frac{q-1}{q} \right)^{-\frac{1}{q-1}}. \tag{3.13}$$

Finally, substituting the result in (3.13) into eq(3.12) we find that the probabilities are equiprobable, i.e. $p_n = 1/W$, and this in turn gives us an expression for the entropy:

$$S_q^{MC} = \frac{W^{1-q} - 1}{1 - q} \tag{3.14}$$

Taking the limit of S_q^{MC} as $q \to 1$ we obtain:

$$\begin{aligned}
\lim_{q\to 1} S_q^{MC} &= \lim_{q\to 1} \frac{W^{1-q} - 1}{1 - q}, \\
S_1^{MC} &= \lim_{q\to 1} \frac{e^{(q-1)\ln W} - 1}{1 - q}, \\
&= \lim_{q\to 1} \frac{\left[1 + (1-q)\ln W + \frac{[(1-q)\ln W]^2}{2} + \frac{[(1-q)\ln W]^3}{6} + \ldots\right] - 1}{1 - q}, \\
&= \lim_{q\to 1} \left[\ln W + \frac{(1-q)\,(\ln W)^2}{2} + \frac{(1-q)^2\,(\ln W)^3}{6} + \ldots\right], \\
&= \ln W.
\end{aligned} \tag{3.15}$$

Thus from the above result it is clear that there is a natural generalization of the familiar logarithm into Tsallis statistics, namely:

$$\ln_q(x) = \frac{x^{1-q} - 1}{1 - q}. \tag{3.16}$$

Furthermore, given (3.16) the associated generalization of the exponential would be:

$$\exp_q(x) = [1 + (1-q)x]^{-\frac{1}{q-1}}, \tag{3.17}$$

where it can be shown in an analogous manner to the analysis performed in (3.15) that $\exp_1(x) = \exp(x)$.

3.2 Canonical Ensemble

We can also adopt the extremization approach in order to generate the Tsallis statistics within the canonical framework. It was quite apparent that in addition to the constraint expressed in (3.10) we require the additional constraint that:

$$\begin{aligned} g &= \sum_{i=1}^{W} p_i E_i \\ &= \bar{E} \end{aligned} \tag{3.18}$$

Using this approach we derive the solve the following variational problem:

$$\delta \left[S(\{p_i\}) - \alpha f - \beta g \right] = 0. \tag{3.19}$$

This gives W equations of the form:

$$\begin{aligned} \frac{q p_n^{q-1}}{q-1} &= \alpha + \beta E_n, \\ p_n &= \left(\frac{q-1}{q} \right)^{\frac{1}{q-1}} \alpha^* \left(1 + \beta^* E_n \right)^{\frac{1}{q-1}}, \end{aligned} \tag{3.20}$$

where $\alpha^* = \alpha^{\frac{1}{q-1}}$ and $\beta^* = \frac{\beta}{\alpha}$. Using the constraint expressed in (3.11) we get that

$$\alpha^* = \frac{\left(\frac{q}{q-1} \right)^{\frac{1}{q-1}}}{\sum_i \left(1 + \beta^* E_i \right)^{\frac{1}{q-1}}} \tag{3.21}$$

From this the expression for the probability of being in a particular state is given by:

$$p_n = \frac{\left(1 + \beta^* E_n \right)^{\frac{1}{q-1}}}{\sum_i \left(1 + \beta^* E_i \right)^{\frac{1}{q-1}}} \tag{3.22}$$

Let $\beta^* \to \beta^*/(q-1)$, this gives:

$$p_n = \frac{\left(1 + (q-1)\beta^* E_n \right)^{\frac{1}{q-1}}}{Z_q} \tag{3.23}$$

where $Z_q \equiv \sum_i (1+(q-1)\beta^* E_i)^{\frac{1}{q-1}}$. Having done this manipulation we can see that (3.23) recovers the usual Boltzmann probability function in the limit $q \to 1$. Furthermore, it is clear that (3.23) depends on the system energy as a power law instead of the usual exponential when $q \neq 1$. However, this approach to maximizing the entropy is shown to produce many a difficulties [15]. The problem is remedied using a different constraint for the average energy; namely,

$$\begin{aligned} g &= \sum_{i=1}^{W} p_i^q E_i \\ &= \bar{E} \end{aligned} \tag{3.24}$$

With the constraint in (3.24) the W equations obtained in the maximisation of the entropy are given:

$$\begin{aligned} \frac{q p_n^{q-1}}{q-1} &= \alpha + \beta q p_n^{q-1} E_n, \\ p_n &= \left[\frac{\alpha(q-1)}{q}\right]^{\frac{1}{q-1}} \left[1+(1-q)\beta E_n\right]^{\frac{1}{1-q}}, \end{aligned} \tag{3.25}$$

where $n = [1, W], n \in \mathbb{N}$. Using the constraint expressed in (3.10) we get that:

$$\left[\frac{\alpha(q-1)}{q}\right]^{-\frac{1}{q-1}} = \sum_i \left[1+(1-q)\beta E_i\right]^{\frac{1}{1-q}} \tag{3.26}$$

Using condition (3.26) in (3.25), the expression for the probability function is:

$$p_n = \frac{\left[1+(1-q)\beta E_n\right]^{\frac{1}{1-q}}}{Z_q}, \tag{3.27}$$

where $Z_q = \sum_i^W \left[1-(q-1)\beta E_i\right]^{-\frac{1}{q-1}}$. If we make the transformation $\beta \to -\beta$ then,

$$\begin{aligned} p_n &= \frac{\left[1-(1-q)\beta E_n\right]^{\frac{1}{1-q}}}{Z_q} \\ &= \frac{\exp_q(-\beta E_n)}{Z_q} \end{aligned} \tag{3.28}$$

This Tsallis representation of the canonical probability distribution looks very much like that derived using Boltzmann statistics and as before the expression in (3.27) retrieves Boltzmann statistics in the limit $q \to 1$ with the probability depending on the system energy as a power law instead of the usual exponential. Using this constraint resolves a lot of problems introduced by using the intuitive constraint expressed in (3.18). The above expression has an energy cutt-off, i.e. a maximal internal energy for which the probability of that particular state is non negative, for $q < 1$ and of course there is no cutt-off for $q > 1$.

3.3 Grand Canonical Ensemble

Just as it turned out that in the canonical formalism of Tsallis statistics that the constraint expressed in (3.18) did not produce desirable characteristics in the derived physics, so it also turns out that in the Grand canonical formalism the constraint on the average number of particles is:

$$\begin{aligned} h &= \sum_{i=1}^{W} p_i^q N_i \\ &= \bar{N} \end{aligned} \tag{3.29}$$

Using the constraint expressed in (3.29) along with the constraints in (3.10) and (3.24), the equation to be solved is:

$$\delta \left[S(\{p_i\}) - \alpha f - \beta g - \gamma h \right] = 0. \tag{3.30}$$

Taking the exact same approach as in the canonical approach the probability of a particular state is given by[1]:

$$p_n = \frac{\left[1 + (q-1)(\beta E_n + \gamma N)\right]^{\frac{1}{1-q}}}{\sum_{N=0}^{\infty} \sum_i \left[1 + (q-1)(\beta E_i + \gamma N)\right]^{\frac{1}{1-q}}}. \tag{3.31}$$

[1]Once again the index $i(n)$ is now representative of macrostate defined by its energy $E_i(E_n)$ as opposed to being representative of a unique configuration of the system (microstate).

It is clear that $p_n = \exp_q\{-\beta(E_i + \mu N)\}/Z_q$ where $\gamma = \beta\mu$ and
$Z_q = \sum_{N=0}^{\infty}\sum_i [1 + (q-1)(\beta E_i + \gamma N)]^{\frac{1}{1-q}}$.
When the SG entropy was used to reproduce BG statistics the discrete probability distribution/s derived depended on the energy and number of particles as an exponential. We could take advantage of this exponential dependence and consider the case of discrete energy levels which eventually gave us the product of multiple exponentials in our partition function and from this we could derive expressions for the average occupation number. Once we obtained the average occupation number we used the large volume approximation to determine the average number of particles in the system. Unfortunately with the Tsallis distribution we cannot use the same approach as the discrete probability distribution depends on the energy and number of particles as a power law and not as an exponential and as such we cannot factor out the exponential associated with each energy level. Instead we get the expression:

$$p_i = \frac{\left[1 + (q-1)(-\beta\sum_{\nu}(n_\nu\epsilon_\nu + \mu n_\nu)\right]^{\frac{1}{1-q}}}{Z_q}, \tag{3.32}$$

where now $Z_q = \sum_{N=0}^{\infty}\sum_i [1 + (q-1)(-\beta\sum_\nu (n_\nu\epsilon_\nu + \mu n_\nu))]^{\frac{1}{1-q}}$. We can see now that each factor of: $-\beta(n_\nu\epsilon_\nu + \mu n_\nu)$ cannot be separated from the other when in the power, i.e.:

$$(A+B)^n \neq A^n + B^n. \tag{3.33}$$

With such an intractable expression, we cannot hope to obtain an expression for the average occupation number and as such an integral form for the average particle number in our gas[2]. We thus require a different approach. Considering (2.26), a possible generalization of (2.26) we can postulate that the entropy as a function of

[2]Under the assumptions of a dilute gas, [20] proceeds to factorize (3.32), in the manner described in (3.33) with the justification that particle correlations may be ignored.

the occupation number is given by[1]:

$$S_q^B = -\sum_\nu \left[n_\nu^q \ln_q n_\nu - n_\nu\right], \tag{3.34}$$

It is evident that in the limit $q \to 1$ (3.34) tends to the familiar Boltzmann-Gibbs entropy expressed in terms of the average occupation number[3], i.e.:

$$S_1^B = -\sum_\nu \left[n_\nu \ln n_\nu - n_\nu\right]. \tag{3.35}$$

We now maximise this entropy subject to the two constraints:

$$g = \sum_\nu n_\nu^q \epsilon_\nu = \bar{E}, \tag{3.36}$$

$$h = \sum_\nu n_\nu^q = \bar{N}. \tag{3.37}$$

Now the equation describing the maximisation condition is given by:

$$\delta\left[S_q^B(\{n_\nu\}) - \beta g - \gamma h\right] = 0. \tag{3.38}$$

This gives several equations for $\nu = i$ where i is a whole number between (and including) the zeroth and last energy level, i.e.:

$$\frac{1 - q n_i^{q-1}}{1-q} - 1 = \beta q n_i^{q-1} \epsilon_i + \gamma q n_i^{q-1}. \tag{3.39}$$

Solving for n_i the following expression is obtained:

$$n_i = \left[1 + \beta(q-1)(\epsilon_i - \mu)\right]^{\frac{1}{1-q}}, \tag{3.40}$$

where $\gamma \equiv -\beta\mu$. Substituting (3.40) back into (3.34) and taking the large volume

[3]Check appendix A.

approximation, this gives:

$$S_q^B = gV \int \frac{d^3p}{(2\pi)^3} \left\{ [1+\beta(q-1)(\epsilon-\mu)]^{\frac{q}{1-q}} \left[\frac{[1+\beta(q-1)(\epsilon-\mu)]^{\frac{1-q}{1-q}} - 1}{q-1} \right] \right.$$
$$\left. + [1+\beta(q-1)(\epsilon-\mu)]^{\frac{1}{1-q}} \right\}, \tag{3.41}$$
$$= gV \int \frac{d^3p}{(2\pi)^3} \beta(\epsilon-\mu) \left[1+\beta(q-1)(\epsilon-\mu)\right]^{\frac{q}{1-q}}$$
$$+ gV \int \frac{d^3p}{(2\pi)^3} \left[1+\beta(q-1)(\epsilon-\mu)\right]^{\frac{1}{1-q}}. \tag{3.42}$$

From (3.42) it is evident that the first term gives $\bar{E}/T$ and $-\mu\bar{N}/T$ respectively. It is not at all obvious what the second term should represent. Let us consider the second term in (3.42), naming it, I_2. Now if we convert to spherical coordinates integral I_2 is expressible in the following form:

$$I_2 = gV(4\pi) \int \frac{dp}{(2\pi)^3} p^2 \left[1+\beta(q-1)(\epsilon-\mu)\right]^{\frac{1}{1-q}}. \tag{3.43}$$

Performing integration by parts on (3.43) and using the relation $\frac{d\epsilon}{dp} = \frac{p}{\epsilon}$, the following is obtained::

$$I_2 = gV \frac{4\pi}{3(2\pi)^3} p^3 \beta \left[1+\beta(q-1)(\epsilon-\mu)\right]^{\frac{1}{1-q}} \Big|_0^\infty$$
$$+ gV \frac{4\pi}{(2\pi)^3} \int_0^\infty dp \frac{p^4}{3\epsilon} \left[1+\beta(1-q)(\epsilon-\mu)\right]^{\frac{q}{1-q}}. \tag{3.44}$$

Let us require that the first term in (3.44) - let us call it $I_{2,1}$ - vanish at the boundaries. It is clear that $I_{2,1}$ vanishes at zero; however, it is evident that there must be some condition imposed on q to ensure $I_{2,1}$ vanish at infinty. As $p \to \infty$, the behaviour of

$I_{2,1}$ can be approximated , i.e.:

$$\begin{aligned} I_{2,1} &= gV\frac{4\pi}{3(2\pi)^3}p^3\left[1+(q-1)\frac{E-\mu}{T}\right]^{-\frac{1}{q-1}}, \\ &\approx gV\frac{4\pi}{3(2\pi)^3}p^3\left[1+(q-1)\frac{p}{T}\right]^{-\frac{1}{q-1}}, \\ &\approx gV\frac{4\pi}{3(2\pi)^3}p^3\left[(q-1)\frac{p}{T}\right]^{-\frac{1}{q-1}}, \\ &= \alpha p^{3-\frac{1}{q-1}}, \end{aligned} \tag{3.45}$$

where $\alpha = gV4\pi/\left(3(2\pi)^3\right)\left[(q-1)/T\right]^{-\frac{1}{q-1}}$. We thus have a condition on q necessary for the first term on the right of the equation to vanish at infinity, namely $3-\frac{1}{q-1}<0$, which gives:

$$1 < q < \frac{4}{3}. \tag{3.46}$$

Given the condition on q, imposed by (3.46), it is evident that $I_{2,1}=0$. Consequently (3.44) simplifies to:

$$I_2 = gV\frac{4\pi}{(2\pi)^3}\int_0^\infty dp\frac{p^3}{3}\frac{p}{\epsilon}\left[1+\beta(q-1)(\epsilon-\mu)\right]^{\frac{q}{1-q}}.$$

Converting back to cartesian coordinates, I_2 becomes:

$$I_2 = gV\int\frac{d^3p}{(2\pi)^3}\frac{p^2}{3\epsilon}\left[1+\beta(q-1)(\epsilon-\mu)\right]^{\frac{q}{1-q}}$$

From our previous prescription for the average number of particles and average energy we can define this term as the pressure times the volume divided by the temperature, i.e. $I_2 = PV/T$.[4]. Thus the entropy is given by:

$$S = \frac{\bar{E}-\mu\bar{N}+PV}{T} \tag{3.47}$$

Furthermore since we assume that the volume is homogeneous we can simply divide

[4]Appendix B alludes to the justification of I_2 being identified in this manner.

all of (3.47) through by the volume to give the densities of the various quantities, i.e.:

$$s = \frac{\epsilon - \mu n + P}{T} \tag{3.48}$$

where s, ϵ and n are the entropy density, energy denisty and number density respectively. But the relations described by (3.47) and (3.48) are precisely the relations we obtain from thermodynamics. We obviously require the entropy to be finite and thus the integrand to be convergent and as a result this places a further condition on q. Let us name the integrand in (3.42) (in spherical coorindates) I. Ignoring the prefactor, $\frac{gV4\pi}{(2\pi)^3}$ (which is inconsequential to such a dimensional analysis) we have that:

$$\begin{aligned} I = p^2\beta(\sqrt{p^2+m^2}-\mu)\left[1+\beta(q-1)(\sqrt{p^2+m^2}-\mu)\right]^{\frac{q}{1-q}}, \\ + \frac{p^4}{3\sqrt{p^2+m^2}}\left[1+\beta(q-1)(\sqrt{p^2+m^2}-\mu)\right]^{\frac{q}{1-q}}. \end{aligned}$$

We may now estimate I for large p, i.e. $p >> 1$:

$$\begin{aligned} I &\approx \beta^{\frac{1}{1-q}}(q-1)^{\frac{q}{1-q}}p^{\frac{3-2q}{1-q}} + \frac{[\beta(q-1)]^{\frac{q}{q-1}}}{3}p^{\frac{3-2q}{1-q}}, \\ &= \alpha p^{\frac{3-2q}{1-q}}, \end{aligned}$$

where $\alpha = \beta^{\frac{1}{1-q}}(q-1)^{\frac{q}{1-q}} + [\beta(q-1)]^{\frac{q}{q-1}}/3$. This gives the restriction $3 - \frac{q}{q-1} < -1$. Consequently, this produces precisely the same constraint on q given by the inequality in (3.46). Incidentally, the constraint we placed on q in order for the first term of I_2 to vanish at the boundaries, derived in (3.46), also ensures that the integrand I, is convergent.

3.4 Thermodynamic Consistency

Classical thermodynamics is characterised by four general thermodynamic laws (from zeroth to third) which describe the universal behaviour of any system irrespective of

the details of microscopic mechanisms. It is exactly this universality, which makes models based on this minimum of information so attractive in the analysis of physical systems emerging from rather complex dynamical evolutions [21].

We have shown in (3.47) and (3.48) that the expression we obtain for entropy is consistent with that of thermodynamics. The most fundamental requirement of a thermostatistical formalism is that it be thermodynamically consistent Thus in order to have thermodynamic consistency we must also fulfil the following relations:

$$n = \left.\frac{\partial P}{\partial \mu}\right|_T, \tag{3.49}$$

$$s = \left.\frac{\partial P}{\partial T}\right|_n, \tag{3.50}$$

$$\mu = \left.\frac{\partial \epsilon}{\partial n}\right|_s, \tag{3.51}$$

$$T = \left.\frac{\partial \epsilon}{\partial s}\right|_n. \tag{3.52}$$

We are now left with the task of ascertaining if the above relations hold true for our statistics and as such conclude if this generalised statistics is thermodynamically consistent. Checking (3.49) we carry out the partial differentiation explicitly, i.e.:

$$\begin{aligned}\frac{\partial P}{\partial \mu} &= \frac{\partial}{\partial \mu}\int \frac{d^3p}{(2\pi)^3}\frac{p^2}{3E}\left[1+(q-1)\frac{E-\mu}{T}\right]^{-\frac{q}{q-1}} \\ &= \int \frac{d^3p}{(2\pi)^3}\frac{p^2}{3E}\frac{q}{T}\left[1+(q-1)\frac{E-\mu}{T}\right]^{-\frac{q}{q-1}-1}\end{aligned} \tag{3.53}$$

but,

$$\frac{\partial}{\partial \mu}\left[1+(q-1)\frac{E-\mu}{T}\right]^{-\frac{q}{q-1}} = -\frac{\partial}{\partial E}\left[1+(q-1)\frac{E-\mu}{T}\right]^{-\frac{q}{q-1}} \tag{3.54}$$

Converting (3.53) to spherical coordinates in momentum space, performing the integral over the angles and using the relation in (3.54) we obtain the following expression:

$$\frac{\partial P}{\partial \mu} = -\int \frac{dp 4\pi}{(2\pi)^3}\frac{p^4}{3E}\frac{\partial}{\partial E}\left[1+(q-1)\frac{E-\mu}{T}\right]^{-\frac{q}{q-1}} \tag{3.55}$$

but $pdp = EdE$; therefore, (3.55) becomes,

$$\frac{\partial P}{\partial \mu} = -\int \frac{dp4\pi}{(2\pi)^3}\frac{p^3}{3}\frac{\partial}{\partial p}\left[1+(q-1)\frac{E-\mu}{T}\right]^{-\frac{q}{q-1}}$$

We can now use integration by parts on the above to give:

$$\frac{\partial P}{\partial \mu} = -\frac{p^3}{3}\left[1+(q-1)\frac{E-\mu}{T}\right]^{-\frac{q}{q-1}}\Bigg|_0^\infty + \int \frac{dp4\pi}{(2\pi)^3}\left(\frac{p^3}{3}\right)\left[1+(q-1)\frac{E-\mu}{T}\right]^{-\frac{q}{q-1}} \tag{3.56}$$

It is clear that the first term on the right of (3.56) vanishes when evaluated at zero, and by our previous requirement on the convergence of (3.42) it should be something finite at infinity. We can check exactly what it tends to as $p \to \infty$.

$$\begin{aligned} I_{2,1} &= -gV\frac{4\pi}{3(2\pi)^3}p^3\left[1+(q-1)\frac{E-\mu}{T}\right]^{-\frac{1}{q-1}} \\ &\approx \frac{p^3}{3}\left[1+(q-1)\frac{p}{T}\right]^{-\frac{1}{q-1}} \\ &\approx -gV\frac{4\pi}{3(2\pi)^3}p^3\left[(q-1)\frac{p}{T}\right]^{-\frac{1}{q-1}} \\ &= \alpha p^{3-\frac{1}{q-1}} \end{aligned} \tag{3.57}$$

This condition is automatically satisfied by our requirement that the integral vanish at infinity as it should. Thus the first term vanishes and we are left with:

$$= \int \frac{dp4\pi}{(2\pi)^3}p^2\left[1+(q-1)\frac{E-\mu}{T}\right]^{-\frac{q}{q-1}} \tag{3.58}$$

$$= \int \frac{d^3p}{(2\pi)^3}\left[1+(q-1)\frac{E-\mu}{T}\right]^{-\frac{q}{q-1}} \tag{3.59}$$

but this is precisely n, and thus the thermodynamic relation shown in one the equations above is satisfied.

In a similar fashion we can prove the thermodynamic relation in (3.50). We know

that:

$$\left.\frac{\partial P}{\partial T}\right|_{\mu} = \int \frac{d^3p}{(2\pi)^3}\frac{p^2}{3E}\frac{q(E-\mu)}{T}\left[1+(q-1)\frac{E-\mu}{T}\right]^{-\frac{q}{q-1}-1} \tag{3.60}$$

In a similar vein to what was done in (3.54), we can change the derivative to one with respect to E, i.e.

$$\frac{\partial}{\partial T}\left[1+(q-1)\frac{E-\mu}{T}\right]^{-\frac{q}{q-1}} = -\left(\frac{E-\mu}{T}\right)\frac{\partial}{\partial E}\left[1+(q-1)\frac{E-\mu}{T}\right]^{-\frac{q}{q-1}} \tag{3.61}$$

Thus using (3.61) we can show that (3.60) can be written in the following form:

$$\begin{aligned} T\left.\frac{\partial P}{\partial T}\right|_{\mu} = &-\int \frac{d^3p}{(2\pi)^3}\frac{p^2}{3}\frac{\partial}{\partial E}\left[1+(q-1)\frac{E-\mu}{T}\right]^{-\frac{q}{q-1}} \\ &+\int \frac{d^3p}{(2\pi)^3}\frac{p^2\mu}{3E}\frac{\partial}{\partial E}\left[1+(q-1)\frac{E-\mu}{T}\right]^{-\frac{q}{q-1}} \end{aligned} \tag{3.62}$$

again using the fact that $pdp = EdE$, (3.62) becomes,

$$\begin{aligned} T\left.\frac{\partial P}{\partial T}\right|_{\mu} = &-\int \frac{d^3p}{(2\pi)^3}\frac{pE}{3}\frac{\partial}{\partial p}\left[1+(q-1)\frac{E-\mu}{T}\right]^{-\frac{q}{q-1}} \\ &+\int \frac{d^3p}{(2\pi)^3}\frac{p\mu}{3}\frac{\partial}{\partial p}\left[1+(q-1)\frac{E-\mu}{T}\right]^{-\frac{q}{q-1}}. \end{aligned}$$

Converting to spherical coordinates then gives:

$$\begin{aligned} T\left.\frac{\partial P}{\partial T}\right|_{\mu} = &-\frac{4\pi}{(2\pi)^3}\int dp\frac{p^3E}{3}\frac{\partial}{\partial p}\left[1+(q-1)\frac{E-\mu}{T}\right]^{-\frac{q}{q-1}} \\ &+\frac{4\pi}{(2\pi)^3}\int dp\frac{p^3\mu}{3}\frac{\partial}{\partial p}\left[1+(q-1)\frac{E-\mu}{T}\right]^{-\frac{q}{q-1}} \end{aligned} \tag{3.63}$$

Using the fact that $\frac{\partial E}{\partial p} = \frac{p}{E}$ and integration by parts, (3.63) becomes:

$$\begin{aligned} T\left.\frac{\partial P}{\partial T}\right|_{\mu} = &- \frac{p^3 E}{3}\left[1+(q-1)\frac{E-\mu}{T}\right]^{-\frac{q}{q-1}}\Bigg|_0^{\infty} \\ &+ \frac{4\pi}{(2\pi)^3}\int_0^{\infty} dp p^2 E\left[1+(q-1)\frac{E-\mu}{T}\right]^{-\frac{q}{q-1}} \\ &+ \frac{4\pi}{(2\pi)^3}\int_0^{\infty} dp \frac{p^4}{3E}\left[1+(q-1)\frac{E-\mu}{T}\right]^{-\frac{q}{q-1}} \\ &+ \frac{4\pi}{(2\pi)^3}\frac{p^3}{3}\left[1+(q-1)\frac{E-\mu}{T}\right]^{-\frac{q}{q-1}}\Bigg|_0^{\infty} \\ &- \frac{4\pi}{(2\pi)^3}\int_0^{\infty} dp p^2 \mu\left[1+(q-1)\frac{E-\mu}{T}\right]^{-\frac{q}{q-1}} \end{aligned} \tag{3.64}$$

The first and fourth terms are zero for the same reasons as discussed previously, and the remaining terms are:

$$\begin{aligned} T\left.\frac{\partial P}{\partial T}\right|_{\mu} &= + \int \frac{d^3 p}{(2\pi)^3} E\left[1+(q-1)\frac{E-\mu}{T}\right]^{-\frac{q}{q-1}} \\ &\quad + \int \frac{d^3 p}{(2\pi)^3}\frac{p^2}{3E}\left[1+(q-1)\frac{E-\mu}{T}\right]^{-\frac{q}{q-1}} \\ &\quad - \frac{d^3 p}{(2\pi)^3} p^2 \mu\left[1+(q-1)\frac{E-\mu}{T}\right]^{-\frac{q}{q-1}} \\ &= \epsilon + P - \mu n \\ &= sT \end{aligned}$$

This proves the thermodynamic relation (Gibbs relation) in (3.50).

In order to prove relation (3.51), it should be noted that we cannot perform the partial integration of ϵ with respect to n directly. As such we need to use the fact that:

$$\begin{aligned} \frac{\partial \epsilon}{\partial n} &= \frac{\frac{\partial \epsilon}{\partial T} dT + \frac{\partial \epsilon}{\partial \mu} d\mu}{\frac{\partial n}{\partial T} dT + \frac{\partial n}{\partial \mu} d\mu} \\ &= \frac{\frac{\partial \epsilon}{\partial T} + \frac{\partial \epsilon}{\partial \mu}\frac{d\mu}{dT}}{\frac{\partial n}{\partial T} + \frac{\partial n}{\partial \mu}\frac{d\mu}{dT}} \end{aligned} \tag{3.65}$$

Furthermore, since s is being held constant, i.e. $ds = 0$ we have that:

$$\frac{\partial s}{\partial T}dT + \frac{\partial s}{\partial \mu}d\mu = 0. \tag{3.66}$$

Rearranging (3.67) gives:

$$\frac{d\mu}{dT} = -\frac{\frac{\partial s}{\partial T}}{\frac{\partial s}{\partial \mu}} \tag{3.67}$$

We can now perform all the derivatives. They are given by the following:

$$\frac{\partial \epsilon}{\partial T} = g\int \frac{d^3p}{(2\pi)^3} qE\left(\frac{E-\mu}{T^2}\right)\left[1+(q-1)\left(\frac{E-\mu}{T}\right)\right]^{-\frac{q}{q-1}-1} \tag{3.68}$$

$$\frac{\partial \epsilon}{\partial \mu} = g\int \frac{d^3p}{(2\pi)^3} \frac{qE}{T}\left[1+(q-1)\left(\frac{E-\mu}{T}\right)\right]^{-\frac{q}{q-1}-1} \tag{3.69}$$

$$\frac{\partial n}{\partial T} = g\int \frac{d^3p}{(2\pi)^3} q\left(\frac{E-\mu}{T^2}\right)\left[1+(q-1)\left(\frac{E-\mu}{T}\right)\right]^{-\frac{q}{q-1}-1} \tag{3.70}$$

$$\frac{\partial n}{\partial \mu} = g\int \frac{d^3p}{(2\pi)^3} \frac{q}{T}\left[1+(q-1)\left(\frac{E-\mu}{T}\right)\right]^{-\frac{q}{q-1}-1} \tag{3.71}$$

$$\frac{\partial s}{\partial T} = g\int \frac{d^3p}{(2\pi)^3} q\left(\frac{E-\mu}{T}\right)\left(\frac{E-\mu}{T^2}\right)\left[1+(q-1)\left(\frac{E-\mu}{T}\right)\right]^{-\frac{q}{q-1}-1} \tag{3.72}$$

$$\frac{\partial s}{\partial \mu} = g\int \frac{d^3p}{(2\pi)^3} \frac{q}{T}\left(\frac{E-\mu}{T}\right)\left[1+(q-1)\left(\frac{E-\mu}{T}\right)\right]^{-\frac{q}{q-1}-1} \tag{3.73}$$

With the expressions in (3.68)-(3.73), and using (3.67) we can explicitly calculate the right hand side of (3.66). In order to make the calculations less cumbersome we define the following variables:

$$x \equiv \frac{E-\mu}{T}\left[1+(q-1)\left(\frac{E-\mu}{T}\right)\right]^{-\frac{q}{q-1}} \tag{3.74}$$

$$y \equiv \frac{1}{T}\left[1+(q-1)\left(\frac{E-\mu}{T}\right)\right]^{-\frac{q}{q-1}} \tag{3.75}$$

$$z \equiv \left[1+(q-1)\left(\frac{E-\mu}{T}\right)\right]^{-1} \tag{3.76}$$

As such we can rewrite the numerator of the right hand side of (3.66) in terms of our newly defined variables, i.e.:

$$\begin{aligned} N &= \int \frac{d^3p}{(2\pi)^3} qExz - \frac{\int \frac{d^3p}{(2\pi)^3} qEyz \int \frac{d^3p}{(2\pi)^3} \left(\frac{E-\mu}{T}\right) xz}{\int \frac{d^3p}{(2\pi)^3} \left(\frac{E-\mu}{T}\right) yz} \\ &= \frac{\int \frac{d^3p}{(2\pi)^3} qExz \int \frac{d^3p}{(2\pi)^3} \left(\frac{E-\mu}{T}\right) yz - \int \frac{d^3p}{(2\pi)^3} qEyz \int \frac{d^3p}{(2\pi)^3} \left(\frac{E-\mu}{T}\right) xz}{\int \frac{d^3p}{(2\pi)^3} \left(\frac{E-\mu}{T}\right) yz} \end{aligned} \tag{3.77}$$

We can write the numerator of (3.77) as the sum of double integrals. However, in doing so we must then label each variable under the integral sign according to which integral it is related, i.e.:

$$N = \frac{\int\int \frac{d^3p_1}{(2\pi)^3} \frac{d^3p_2}{(2\pi)^3} qE_1 x_1 z_1 \left(\frac{E_2-\mu}{T}\right) y_2 z_2 - \int\int \frac{d^3p_1}{(2\pi)^3} \frac{d^3p_2}{(2\pi)^3} qE_1 y_1 z_1 \left(\frac{E_2-\mu}{T}\right) x_2 z_2}{\int \frac{d^3p}{(2\pi)^3} \left(\frac{E-\mu}{T}\right) yz} \tag{3.78}$$

From (3.78) it is clear that we can factorise the numerator to give:

$$N = \frac{\int\int \frac{d^3p_1}{(2\pi)^3} \frac{d^3p_2}{(2\pi)^3} qE_1 \left(\frac{E_2-\mu}{T}\right) z_1 z_2 \left(x_1 y_2 - y_1 x_2\right)}{\int \frac{d^3p}{(2\pi)^3} \left(\frac{E-\mu}{T}\right) yz}. \tag{3.79}$$

The denominator in the right hand side of (3.66) can be written in an analogous manner to the numerator in terms of our newly defined variables as:

$$D = \frac{\int\int \frac{d^3p_1}{(2\pi)^3} \frac{d^3p_2}{(2\pi)^3} qx_1 z_1 \left(\frac{E_2-\mu}{T}\right) y_2 z_2 - \int\int \frac{d^3p_1}{(2\pi)^3} \frac{d^3p_2}{(2\pi)^3} qy_1 z_1 \left(\frac{E_2-\mu}{T}\right) x_2 z_2}{\int \frac{d^3p}{(2\pi)^3} \left(\frac{E-\mu}{T}\right) yz}. \tag{3.80}$$

Gathering the like terms in (3.80) gives:

$$D = \frac{\int\int \frac{d^3p_1}{(2\pi)^3} \frac{d^3p_2}{(2\pi)^3} qz_1 z_2 \left(\frac{E_2-\mu}{T}\right) \left(x_1 y_2 - y_1 x_2\right)}{\int \frac{d^3p}{(2\pi)^3} \left(\frac{E-\mu}{T}\right) yz}. \tag{3.81}$$

Thus $\frac{\partial\epsilon}{\partial n}|_s$ is attained by dividing (3.79) by (3.81), i.e.,

$$\begin{aligned}\left.\frac{\partial\epsilon}{\partial n}\right|_s &= \frac{\int\int \frac{d^3p_1}{(2\pi)^3}\frac{d^3p_2}{(2\pi)^3} qE_1\left(\frac{E_2-\mu}{T}\right) z_1z_2\left(x_1y_2-y_1x_2\right)}{\int\int \frac{d^3p_1}{(2\pi)^3}\frac{d^3p_2}{(2\pi)^3} qz_1z_2\left(\frac{E_2-\mu}{T}\right)\left(x_1y_2-y_1x_2\right)}, \\ &= \frac{\int\int \frac{d^3p_1}{(2\pi)^3}\frac{d^3p_2}{(2\pi)^3} q\frac{E_1E_2}{T} z_1z_2\left(x_1y_2-y_1x_2\right) - \int\int \frac{d^3p_1}{(2\pi)^3}\frac{d^3p_2}{(2\pi)^3} q\frac{E_1\mu}{T} z_1z_2\left(x_1y_2-y_1x_2\right)}{\int\int \frac{d^3p_1}{(2\pi)^3}\frac{d^3p_2}{(2\pi)^3} qz_1z_2\frac{E_2}{T}\left(x_1y_2-y_1x_2\right) - \int\int \frac{d^3p_1}{(2\pi)^3}\frac{d^3p_2}{(2\pi)^3} qz_1z_2\frac{\mu}{T}\left(x_1y_2-y_1x_2\right)}.\end{aligned} \tag{3.82}$$

Paying closer attention to (3.82) it becomes clear that the first term in the numerator is zero and the second term in the denominator is zero. This leaves us with:

$$\left.\frac{\partial\epsilon}{\partial n}\right|_s = -\frac{\int\int \frac{d^3p_1}{(2\pi)^3}\frac{d^3p_2}{(2\pi)^3} q\frac{E_1\mu}{T} z_1z_2\left(x_1y_2-y_1x_2\right)}{\int\int \frac{d^3p_1}{(2\pi)^3}\frac{d^3p_2}{(2\pi)^3} qz_1z_2\frac{E_2}{T}\left(x_1y_2-y_1x_2\right)}. \tag{3.83}$$

But the numerator in (3.83) is precisely equal to $-\mu$ multiplied by the denominator of (3.83). Thus we have the result we sought, namely:

$$\left.\frac{\partial\epsilon}{\partial n}\right|_s = \mu. \tag{3.84}$$

In order to prove the relation in (3.52), we use an approach analogues to what we have used to prove (3.51). Just as with (3.51) we note that we cannot perform the partial differentiation directly we write the partial integral in (3.52) as the following:

$$\begin{aligned}\left.\frac{\partial\epsilon}{\partial s}\right|_n &= \frac{\frac{\partial\epsilon}{\partial T}+\frac{\partial\epsilon}{\partial\mu}\frac{d\mu}{dT}}{\frac{\partial n}{\partial T}+\frac{\partial n}{\partial\mu}\frac{d\mu}{dT}} \\ &= \frac{\frac{\partial\epsilon}{\partial T}+\frac{\partial\epsilon}{\partial\mu}\frac{d\mu}{dT}}{\frac{\partial s}{\partial T}+\frac{\partial s}{\partial\mu}\frac{d\mu}{dT}}\end{aligned} \tag{3.85}$$

and since n must be held constant we have the added condition that:

$$\frac{d\mu}{dT} = -\frac{\frac{\partial n}{\partial T}}{\frac{\partial n}{\partial\mu}} \tag{3.86}$$

Using the relations in (3.68)-(3.73) along with the defined variables in (3.74)-(3.76), we can write the numerator of (3.85) as

$$\begin{aligned} N_2 &= \int \frac{d^3p}{(2\pi)^3}\frac{q}{T}Exz - \frac{\int \frac{d^3p}{(2\pi)^3}\frac{q}{T}Eyz \int \frac{d^3p}{(2\pi)^3}xz}{\int \frac{d^3p}{(2\pi)^3}yz}, \\ &= \frac{\frac{q}{T}\int\int \frac{d^3p_1}{(2\pi)^3}\frac{d^3p_2}{(2\pi)^3}E_1 z_1 z_2 \left(x_1 y_2 - y_1 x_2\right)}{\int \frac{d^3p}{(2\pi)^3}yz}. \end{aligned} \tag{3.87}$$

Similarly we can write the denominator as:

$$\begin{aligned} D_2 &= \int \frac{d^3p}{(2\pi)^3}q\frac{E-\mu}{T^2}xz - \frac{\int \frac{d^3p}{(2\pi)^3}\frac{E-\mu}{T^2}yz \int \frac{d^3p}{(2\pi)^3}xz}{\int \frac{d^3p}{(2\pi)^3}yz}, \\ &= \frac{\frac{q}{T^2}\int\int \frac{d^3p_1}{(2\pi)^3}\frac{d^3p_2}{(2\pi)^3}(E_1-\mu) z_1 z_2 \left(x_1 y_2 - y_1 x_2\right)}{\int \frac{d^3p}{(2\pi)^3}yz}. \end{aligned} \tag{3.88}$$

Thus dividing (3.87) by (3.88) we obtain the following expression for $\left.\frac{\partial\epsilon}{\partial s}\right|_n$:

$$\begin{aligned} \left.\frac{\partial\epsilon}{\partial s}\right|_n &= T\frac{\int\int \frac{d^3p_1}{(2\pi)^3}\frac{d^3p_2}{(2\pi)^3}E_1 z_1 z_2 \left(x_1 y_2 - y_1 x_2\right)}{\int\int \frac{d^3p_1}{(2\pi)^3}\frac{d^3p_2}{(2\pi)^3}(E_1-\mu) z_1 z_2 \left(x_1 y_2 - y_1 x_2\right)}, \\ &= T\frac{\int\int \frac{d^3p_1}{(2\pi)^3}\frac{d^3p_2}{(2\pi)^3}E_1 z_1 z_2 \left(x_1 y_2 - y_1 x_2\right)}{\int\int \frac{d^3p_1}{(2\pi)^3}\frac{d^3p_2}{(2\pi)^3}E_1 z_1 z_2 \left(x_1 y_2 - y_1 x_2\right) - \int\int \frac{d^3p_1}{(2\pi)^3}\frac{d^3p_2}{(2\pi)^3}\mu z_1 z_2 \left(x_1 y_2 - y_1 x_2\right)}. \end{aligned} \tag{3.89}$$

Upon closer analysis of (3.89) it is clear that the second term in the denominator is equal to zero. Furthermore the first term in the denominator is identically equal to the term in the numerator. Taking this into consideration the entire fraction is just equal to 1. As such we have that:

$$\left.\frac{\partial\epsilon}{\partial s}\right|_n = T. \tag{3.90}$$

But (3.90) is precisely the relation in (3.52). We have thus proved thermodynamic relation (3.52). Having proved all of the thermodynamic relation, we come to the conclusion that our new form of statistics is thermodynamically consistent. In fact is

is due to the appropriate choice of constraints reflected in (equations) and the correct identification of Lagrange multipliers to intensive quantities that we have been able to obtain a self consistent, thermodynamically consistent formulation for the entropy. Had typical constraints, in which the energy and total number of particles depend linearly on the occupation number, been utilized, it would have turned out that our formulation would have been thermodynamically inconsistent.

It must be noted that neither the formulation of the entropy functional nor the constraints imposed on the total energy, E, nor the total particle number, N, are unique. This is discussed and shown in [22], and it is shown if one chooses the entropy to be given by:

$$S_q = \sum_i C_q \left(n_i^{1/q} \right), \tag{3.91}$$

where $C_q(x)$ is defined as:

$$C_q(x) = \begin{cases} \frac{x-x^q}{q-1} + \frac{(1-x)-(1-x)^q}{q-1} & \text{if } x \leq \frac{1}{2} \\ \frac{x-x^{2-q}}{q-1} + \frac{(1-x)-(1-x)^{2-q}}{q-1} & \text{if } x \geq \frac{1}{2} \end{cases}, \tag{3.92}$$

with linear constraints:

$$E = \sum_i n_i \epsilon_i, \tag{3.93}$$

$$N = \sum_i n_i, \tag{3.94}$$

then precisely the same expression for the average occupation number, n_i, as expressed in (3.40) is obtained, although in [22] thermodynamic consistency is not tested.

Furthermore, one can, very naturally, employ this approach for the case of a gas of fermions or bosons as was done in [1], by generalizing the expression in (2.24) to the following:

$$S_q^{FD,BE} = -\sum_\nu \left[n_\nu^q \ln_q n_\nu \pm (1 \mp n_\nu)^q \ln_q (1 \mp n_\nu) \right]. \tag{3.95}$$

and using the constraints expressed in (3.36) and (3.37), the expression for the average occupation number obtained is,

$$n_i^{FD,BE} = \frac{1}{\exp_q \{-\beta(\epsilon_i - \mu)\} \pm 1}, \tag{3.96}$$

and, although perhaps more technical, this too proves to be thermodynamically consistent.

Chapter 4

Results

The expression for the average number of particles using the Tsallis expression for entropy in (3.34) is given by the average occupancy in (3.59) multiplied by the volume, i.e.:

$$N = gV \int \frac{d^3p}{(2\pi)^3} \left[1 + \beta(q-1)(E-\mu)\right]^{\frac{q}{1-q}} \tag{4.1}$$

Our aim now is to fit transverse momentum spectra using the function in (4.1) such that we may find universal values for the temperature, T, radius, R, assuming a spherical fireball, i.e. $V = \frac{4}{3}\pi R^3$, and q value of the fireball at freeze-out (at given centre of mass energies) for all particle species as well as to possibly find relations between these parameters and the centre of mass energy so as to predict the fireball parameters at untested $\sqrt{s}$ energies and to compare them at lower energies to those already calculated.

Using the fact that $E = m_t \cosh y$ and $p_z = m_t \sinh y$ where m_t and y are the transverse mass and pseudorapidity respectively [1] we can rewrite (4.1) into the following more useful form:

$$N = gV \int \frac{dp_t d\phi dy p_t m_t \cosh y}{(2\pi)^3} \left[1 + \beta(q-1)(m_t \cosh y - \mu)\right]^{\frac{q}{1-q}} \tag{4.2}$$

[1] Check appendix B.

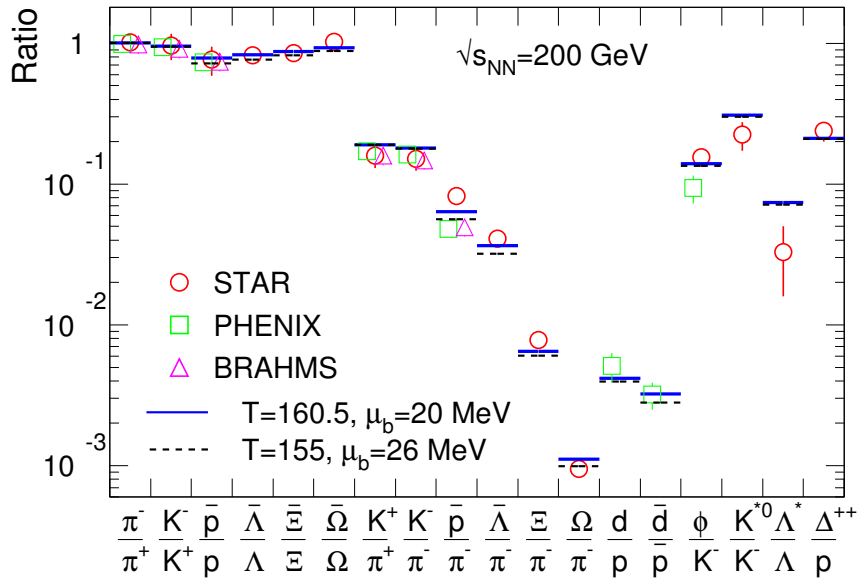

Figure 4.1: Graph, obtained from [4], of particle ratios taken from several experiments at 200 GeV.

and thus integrating over the angle ϕ it follows from (4.2) that the transverse momentum spectrum for our given Tsallis distribution for a static fireball, i.e. no transverse flow, is given by:

$$\frac{d^2N}{dp_t dy} = gV\frac{p_t m_t \cosh y}{(2\pi)^2}\left[1+\beta(q-1)(m_t\cosh y-\mu)\right]^{\frac{q}{1-q}} \tag{4.3}$$

When spectra are evaluated in the central rapidity region, i.e. $y=0$, (4.2) simplifies to:

$$\frac{d^2N}{dp_t dy} = gV\frac{p_t m_t}{(2\pi)^2}\left[1+\beta(q-1)(m_t-\mu)\right]^{\frac{q}{1-q}}. \tag{4.4}$$

All the data fitted here is data taken around the central rapidity region and thus for the purposes of the fits performed, (4.4) is the relevant expression. At LHC energies equal numbers of particles and anti-particles are created, evidence of such can be seen in fig(4.1). This has consequences for the chemical potential. In general

the chemical potential μ_i of some particle species i is given by $\mu_i = \vec{\mu} \cdot \vec{Q}_i$ where $\vec{\mu} = (\mu_Q, \mu_B, \mu_S, \mu_C)$ is the vector chemical potential associated with all the relevant conserved quantum numbers and $\vec{Q}_i = (Q_i, B_i, S_i, C_i)$ is the vector containing the values for all the relevant quantum numbers associated with particle specie i.
Consider the case of a π^+ meson and its antiparticle the π^-. Given that they are equally produced, $\mu_{\pi^+} = \mu_{\pi^-} = -\mu_{\pi^+}$. This resulting condition is $2\mu_Q = \mu_Q = 0$. Furthermore, consider a proton and an anti-proton. Seeing as these too are equally produced then $\mu_p = \mu_{\bar{p}} = -\mu_p$. This resulting condition from this consideration is

$$\begin{aligned} 0 &= 2\mu_B + 2\mu_Q, \\ \mu_B &= -\mu_Q, \end{aligned} \tag{4.5}$$

However, $\mu_Q = 0$, which then implies that $\mu_B = 0$. We can continue to consider particles with a larger number of nonzero quantum numbers so as to come to the conclusion that at high energies the chemical potential for all particle species is very near zero, i.e. $\mu_i \approx 0$ for all i.
Given that we can approximate the chemical potential of all particles within the fireball as zero, the relevant function necessary for fitting the transverse momentum spectrum of particle species i is given by:

$$\frac{d^2N}{dp_t dy} = gV \frac{p_t m_t}{(2\pi)^2} \left[1 + \beta(q-1)m_t\right]^{\frac{q}{1-q}}. \tag{4.6}$$

In the case of the transverse momentum spectra of charged hadrons, the function used to fit the spectra is a combination of that of the pion, kaon, and proton transverse momentum spectra (assuming the contribution from heavier charged hadrons is negligible), i.e.:

$$\begin{aligned} \frac{d^2N}{dp_t dy} = \frac{gVp_t}{(2\pi)^2} \Big\{ & m_{t,\pi}(2\pi)^2 \left[1 + \beta(q-1)m_{t,\pi}\right]^{\frac{q}{1-q}} + m_{t,\mathrm{K}}(2\pi)^2 \left[1 + \beta(q-1)m_{t,\mathrm{K}}\right]^{\frac{q}{1-q}} \\ & + m_{t,\mathrm{p}}(2\pi)^2 \left[1 + \beta(q-1)m_{t,\mathrm{p}}\right]^{\frac{q}{1-q}} \Big\}, \end{aligned} \tag{4.7}$$

where $m_{t,\pi}$, $m_{t,\mathrm{K}}$ and $m_{t,\mathrm{p}}$ are the transverse masses of the pion, kaon, and proton respectively. Similarly, it can be easily verified that the expression for the transverse momentum spectrum for some particle species i, at mid-rapidity for energies characteristic of those at the LHC, using Boltzmann-Gibbs statistics is given by the expression:

$$\frac{d^2N}{dp_t dy} = gV\frac{p_t m_t}{(2\pi)^2}\exp\left\{-\beta m_t\right\}. \tag{4.8}$$

Some p_t spectra show the transverse momentum plotted against $\frac{1}{2\pi p_t}\frac{d^2N}{dp_t d\eta}$. In this case the Tsallis distribution fitted at mid-rapidity is:

$$\frac{1}{2\pi p_t}\frac{d^2N}{dp_t d\eta} = \frac{gV}{(2\pi)^3}p_t\left[1+\beta(q-1)m_t\right]^{\frac{q}{1-q}}. \tag{4.9}$$

Power law distributions have been used in STAR, PHENIX, ATLAS, ALICE and CMS experiments to parametrise various particle spectra. The parametrisation used by these experiments is:

$$\frac{d^2N}{dp_t dy} = p_t\frac{dN}{dy}\frac{(n-1)(n-2)}{nC\left(nC+m_0(n-2)\right)}\left[1+\frac{m_t-m_0}{nC}\right]^{-n}, \tag{4.10}$$

where n, C and $\left.\frac{dN}{dy}\right|_{y=0}$ are the parameters to be fitted.[23] relates the volume to $\frac{dN}{dy}$. We can integrate (4.4) over p_t, i.e.:

$$\left.\frac{dN}{dy}\right|_{y=0} = gV\int_0^\infty dp_t\frac{p_t m_t}{(2\pi)^2}\left[1+\beta(q-1)m_t\right]^{\frac{q}{1-q}}. \tag{4.11}$$

For simplicity, let $\alpha_0 \equiv \frac{gV}{(2\pi)^2}$ and $\alpha_1 \equiv \beta(q-1)$ and $\frac{q}{q-1} \equiv n$. Using this and the fact that $m_t dm_t = p_t dp_t$ the integral can be re-expressed in the following form:

$$\left.\frac{dN}{dy}\right|_{y=0} = \alpha_0\int_{m_0}^\infty m_t^2\left[1+\alpha_1 m_t\right]^{-n} \tag{4.12}$$

Now we let $x \equiv 1 + \alpha_1 m_t$. This gives:

$$\left.\frac{dN}{dy}\right|_{y=0} = \frac{\alpha_0}{\alpha_1^3} \int_{1+\alpha_1 m_0}^{\infty} dx(x-1)^2 x^{-n} \tag{4.13}$$

$$= \frac{\alpha_0}{\alpha_1^3} \left[\frac{1}{3-n}x^{3-n} - \frac{2}{2-n}x^{2-n} + \frac{1}{1-n}x^{1-n}\right]\Bigg|_{1+\alpha_1 m_0}^{\infty} \tag{4.14}$$

Substituting $\alpha_0 = \frac{gV}{(2\pi)^2}$ and $\alpha_1 = \beta(q-1)$ and $\frac{q}{q-1} = n$ into (4.14), the final expression:

$$\left.\frac{dN}{dy}\right|_{y=0} = \frac{gVT}{(2\pi)^2}\left[\frac{(2-q)(3-2q)}{(2-q)m_0^2 + 2m_0T + 2T^2}\right]^{-1}\left[1 + (q-1)\frac{m_0}{T}\right]^{\frac{1}{1-q}}, \tag{4.15}$$

is obtained. Thus the single-species particle spectrum, at mid-rapidity can be expressed as:

$$\left.\frac{d^2N}{dp_t dy}\right|_{y=0} = p_t \left.\frac{dN}{dy}\right|_{y=0} \frac{m_t}{T}\frac{(2-q)(3-2q)}{(2-q)m_0^2 + 2m_0T + 2T^2}\left[1 + (q-1)\frac{m_0}{T}\right]^{\frac{1}{q-1}}\left[1 + (q-1)\frac{m_t}{T}\right]^{-\frac{q}{q-1}} \tag{4.16}$$

This expression obtained using generalized statistics is fairly similar to that of the both statistical mechanics inspired (low p_t) and QCD inspired (high p_t) empirical formula in (4.10), used in [24], [25], [26] and [27].

data set	particle	R (GeV^{-1}),	T (GeV)	q	χ^2/NDF
ALICE pp 900 GeV	π^+	4.84 ± 0.15	0.0703 ± 0.0025	1.1485 ± 0.0056	12.59/30
	π^-	4.74 ± 0.14	0.0719 ± 0.0025	1.1448 ± 0.0055	8.65/30
	p	28 ± 16	0.0248 ± 0.0075	1.1543 ± 0.0071	7.07/21
	$\bar{\text{p}}$	6.5 ± 7.6	0.056 ± 0.039	1.129 ± 0.032	7.01/21
	K^+	4.5 ± 1.7	0.057 ± 0.017	1.174 ± 0.022	6.56/24
	K^-	4.0 ± 1.3	0.064 ± 0.016	1.161 ± 0.020	3.17/24
	Λ	3.1 ± 4.1	0.092 ± 0.071	1.102 ± 0.043	5.54/6
	$\bar{\Lambda}$	5 ± 10	0.066 ± 0.067	1.116 ± 0.041	1.95/6
	ϕ	14 ± 48	0.022 ± 0.044	1.183 ± 0.050	0.49/1
CMS pp 900 GeV	π^+	5.43 ± 0.16	0.0669 ± 0.0021	1.1634 ± 0.0049	3.91/19
	π^-	5.776 ± 0.019	0.06227 ± 0.00022	1.17662 ± 0.00067	18.57/19
	p	4.33 ± 0.12	0.0733 ± 0.0013	1.1241 ± 0.0023	9.34/24
	$\bar{\text{p}}$	5.11 ± 0.15	0.0659 ± 0.0012	1.1286 ± 0.0022	18.55/24
	K^+	3.284 ± 1.072	0.078 ± 0.024	1.158 ± 0.040	1.79/14
	K^-	4.1 ± 2.2	0.063 ± 0.031	1.183 ± 0.053	1.02/14
CMS pp 7 TeV	π^+	6.78 ± 0.26	0.0592 ± 0.0024	1.2031 ± 0.0060	12.15/19
	π^-	6.62 ± 0.24	0.0603 ± 0.0024	1.2018 ± 0.0059	10.11/19
	p	4.10 ± 0.12	0.0699 ± 0.0014	1.1650 ± 0.0030	11.68/24
	$\bar{\text{p}}$	6.62 ± 0.24	0.0603 ± 0.0024	1.2018 ± 0.0059	15.21/24
	K^+	2.65 ± 0.64	0.102 ± 0.026	1.152 ± 0.045	1.75/14
	K^-	3.2 ± 1.5	0.083 ± 0.039	1.186 ± 0.068	3.68/14
CMS pp 900 GeV	charged hadrons	6.66 ± 0.44	0.0701 ± 0.0042	1.1293 ± 0.0051	69.08/21
CMS pp 2360 GeV	charged hadrons	7.57 ± 0.58	0.0656 ± 0.0045	1.1452 ± 0.0057	58.91/21
CMS pp 7 TeV	charged hadrons	7.55 ± 0.41	0.0708 ± 0.0034	1.1479 ± 0.0035	131.36/31
ATLAS pp 900 GeV	charged hadrons	6.0 ± 1.3	0.076 ± 0.010	1.1261 ± 0.0073	56.99/28
ATLAS pp 2360 GeV	charged hadrons	6.30 ± 2.42	0.073 ± 0.019	1.141 ± 0.014	3.11/19
ATLAS pp 7 TeV	charged hadrons	7 ± 16	0.07 ± 0.10	1.152 ± 0.049	70.58/33
ALICE pPb 5020 GeV	charged hadrons	4.94 ± 0.31	0.1182 ± 0.0057	1.1417 ± 0.0032	634.79/42

Table 4.1: Parameter and χ^2/NDF values obtained from Tsallis fits performed on ALICE, CMS and ATLAS data sets at several energies, where R is the fireball radius, T the fireball temperature, and q the Tsallis q value.

particle		T	q	R
π^+	T	1.000	-0.944	-0.984
	q	-0.944	1.000	0.895
π^-	T	1.000	-0.944	-0.984
	q	-0.944	1.000	0.895
p	T	1.000	-0.875	-0.995
	q	-0.875	1.000	0.822
$\bar{\text{p}}$	T	1.000	-0.993	-0.999
	q	-0.993	1.000	0.989
K^+	T	1.000	-0.983	-0.999
	q	-0.983	1.000	0.973
K^-	T	1.000	-0.982	-0.998
	q	-0.982	1.000	0.970
Λ	T	1.000	-0.978	-0.997
	q	-0.978	1.000	0.962
$\bar{\Lambda}$	T	1.000	-0.975	-0.998
	q	-0.975	1.000	0.959
	R	-0.998	0.959	1.000
ϕ	T	1.000	-0.730	-0.986
	q	-0.730	1.000	0.608

Table 4.2: Correlation coefficients for fitted parameters for several hadrons from ALICE pp 900 GeV

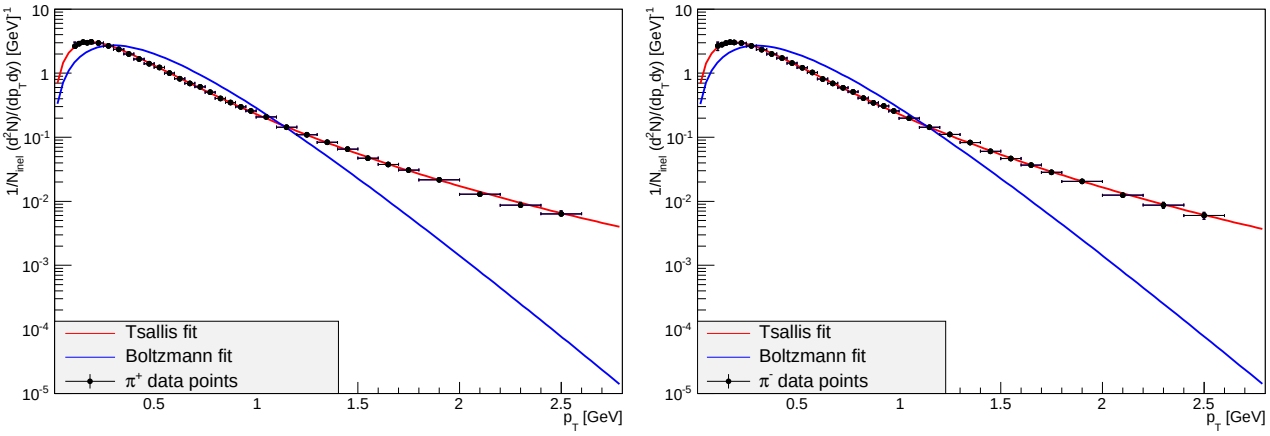

Figure 4.2: Tsallis and Boltzmann fits to p_t spectra for ALICE pp experiment performed at 900GeV for π^+(left panel) and π^-(right panel) mesons. Refer to (4.1) for Tsallis parameter values.

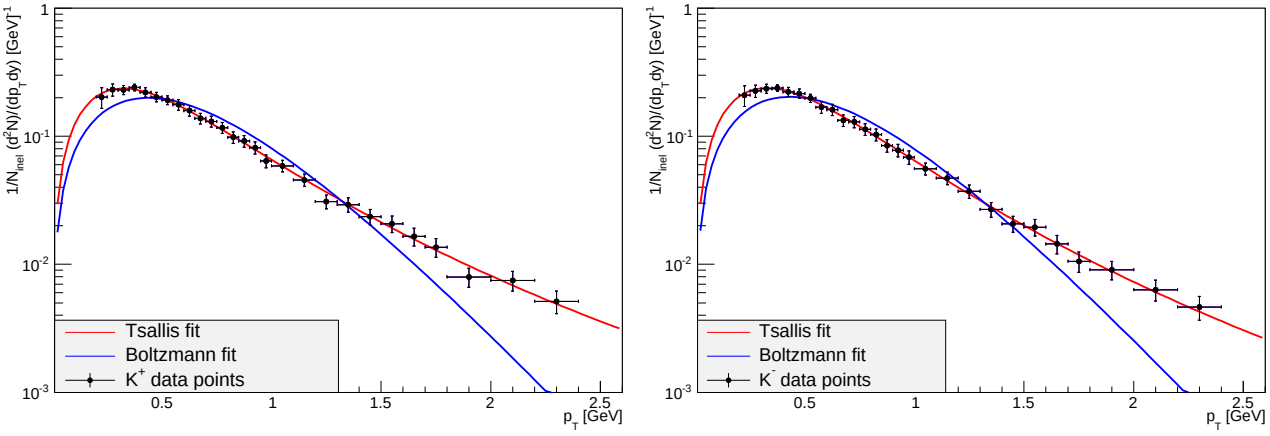

Figure 4.3: Tsallis and Boltzmann fits to p_t spectra for ALICE pp experiment performed at 900GeV for K^+(left panel) and K^-(right panel) mesons. Refer to (4.1) for Tsallis parameter values.

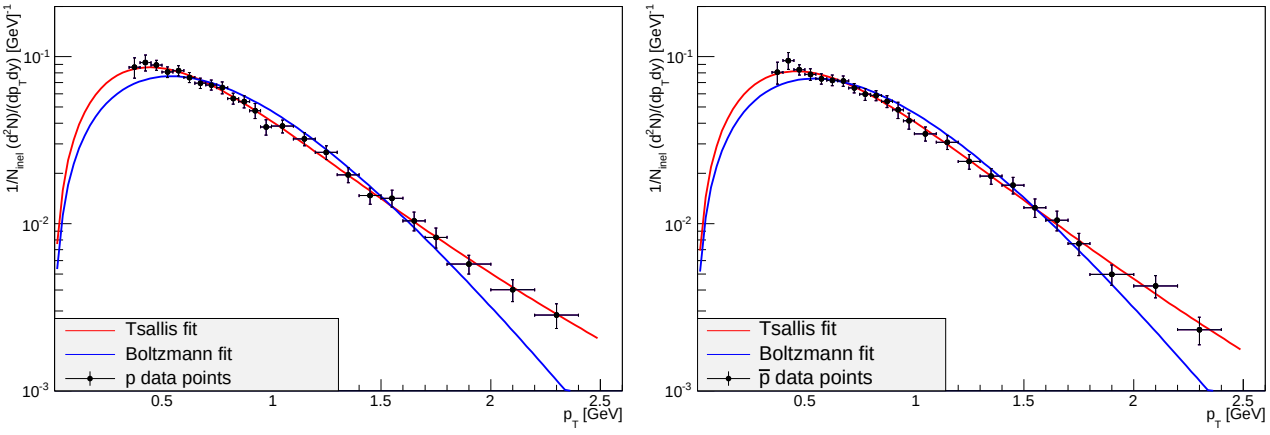

Figure 4.4: Tsallis and Boltzmann fits to p_t spectra for ALICE pp experiment performed at 900GeV for p(left panel) and $\bar{p}$(right panel) baryons. Refer to (4.1) for Tsallis parameter values.

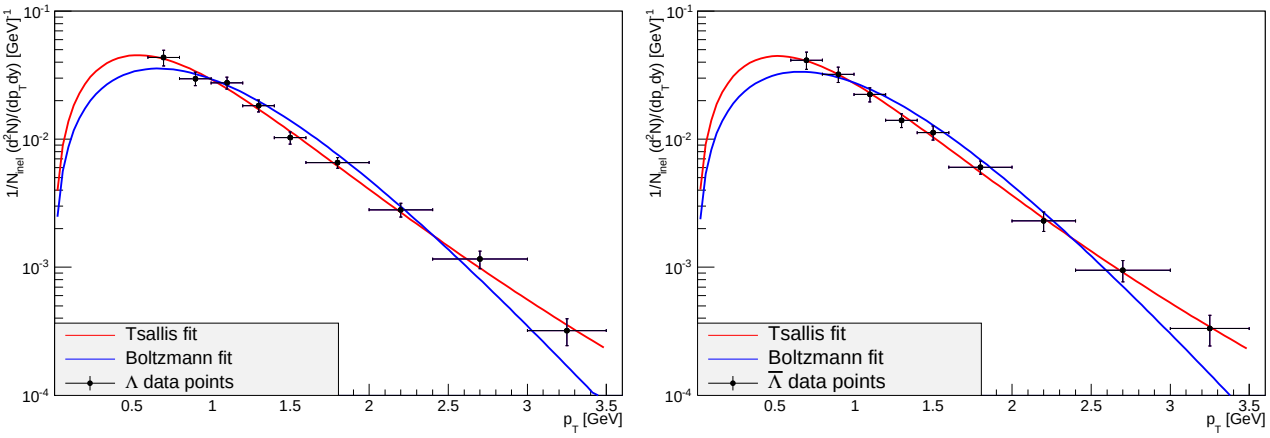

Figure 4.5: Tsallis and Boltzmann fits to p_t spectra for ALICE pp experiment performed at 900GeV for Λ(left panel) and $\bar{\Lambda}$(right panel) baryons. Refer to (4.1) for Tsallis parameter values.

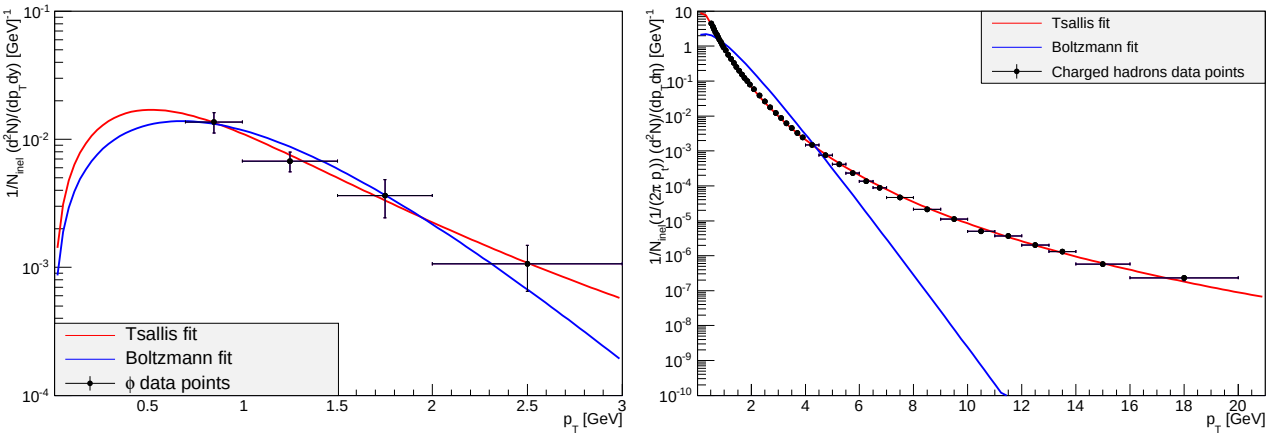

Figure 4.6: Tsallis and Boltzmann fits to p_t spectra for ALICE pp experiment performed at 900 GeV for ϕ meson(left panel) and Tsallis and Boltzmann fits to p_t spectra for ALICE pPb experiment performed at 5020 GeV for charged particles(left panel). Refer to Table(4.1) for Tsallis parameter values.

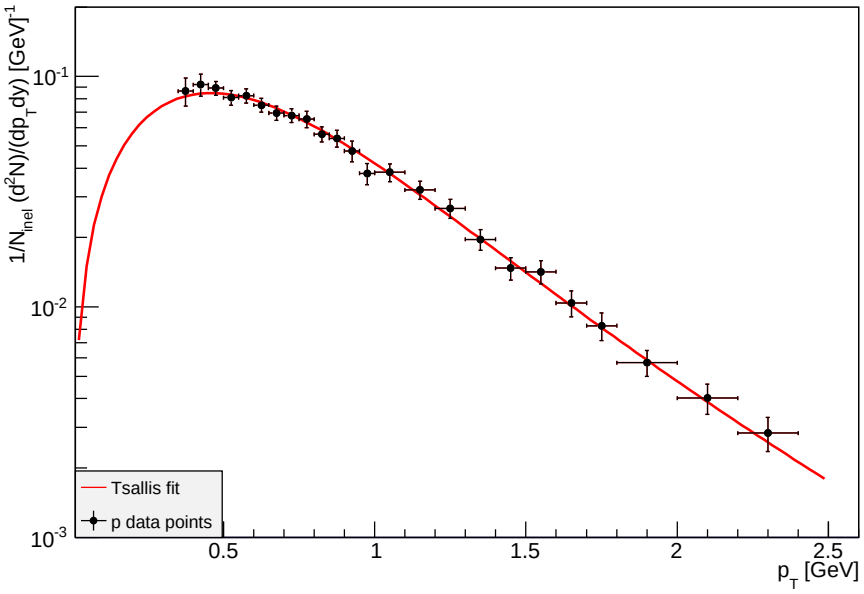

Figure 4.7: Tsallis fit to p_t spectrum for ALICE pp experiment performed at 900GeV for proton, with q value for Tsallis fit fixed to the $q = 1.129$ value obtained from the antiproton spectrum. Fit values obtained for the two remaining parameters were $T = 0.0553 \pm 0.0044\,\mathrm{GeV}$ and $R = 6.8 \pm 1.2\,\mathrm{GeV}^{-1}$ and $\chi^2/\mathrm{NDF} = 7.71675/22$.

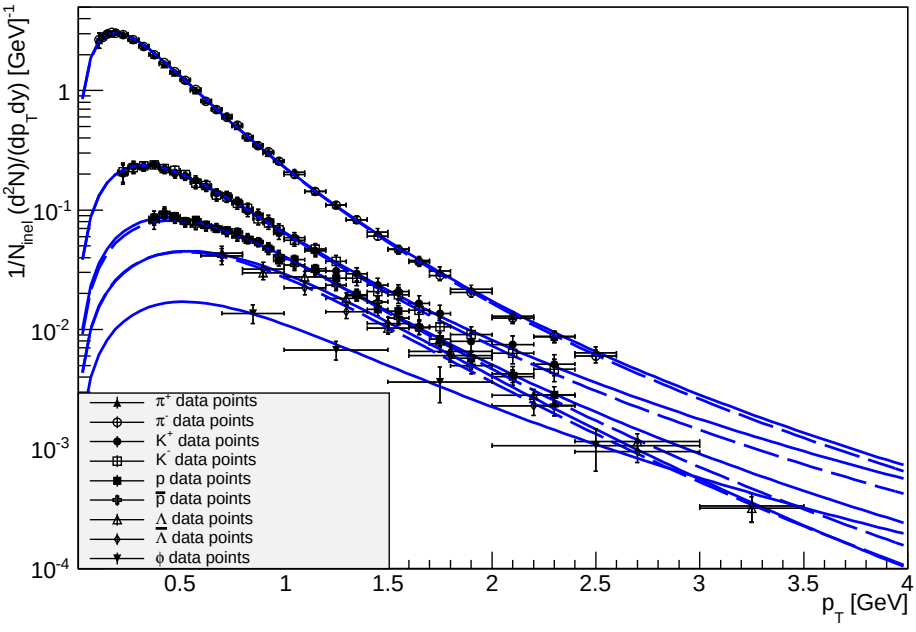

Figure 4.8: Tsallis fit to p_t spectra for π^+, π^-, K^+, K^-, p, $\bar{\mathrm{p}}$, Λ, $\bar{\Lambda}$ and ϕ particles for ALICE pp experiment at 900 GeV. (Anti)Particle fits are shown as (dashed)solid lines.

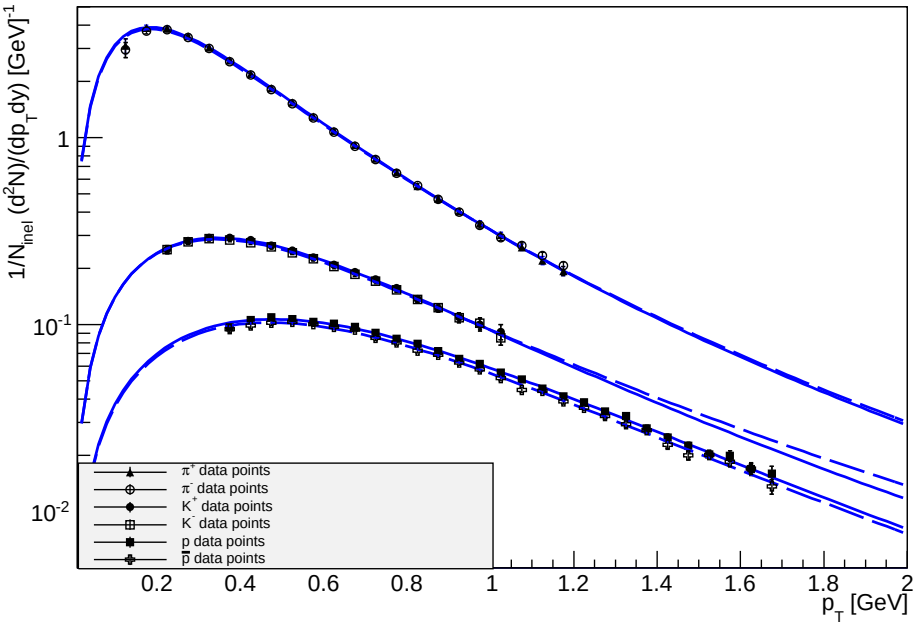

Figure 4.9: Tsallis fit to p_t spectra for π^+, π^-, K^+, K^-, p and $\bar{p}$ particles for CMS pp experiment at 900 GeV. (Anti)Particle fits are shown as (dashed)solid lines.

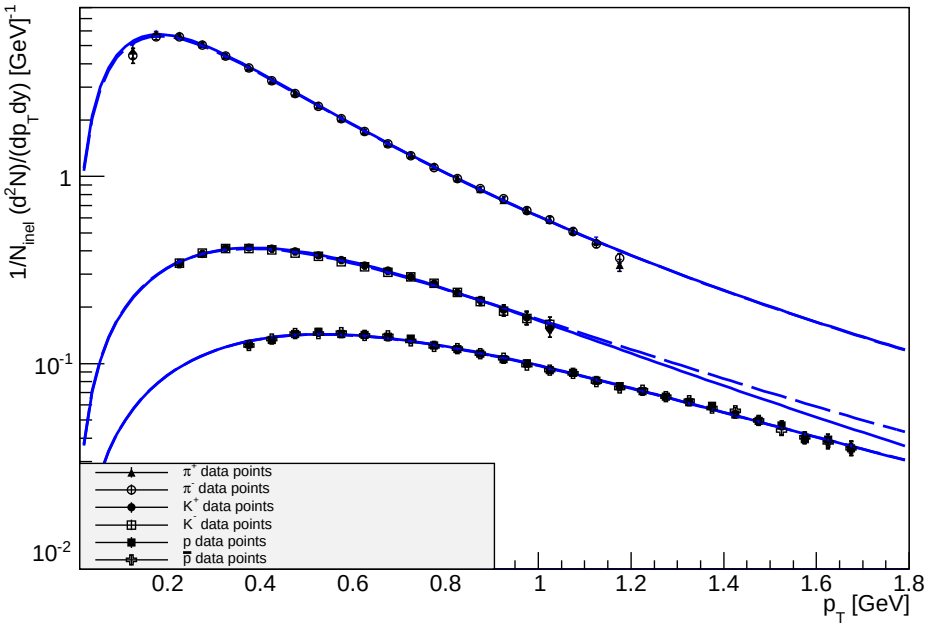

Figure 4.10: Tsallis fit to π^+, π^-, K^+, K^-, p and $\bar{p}$ particles for CMS pp experiment at 7 TeV. (Anti)Particle fits are shown as (dashed)solid lines.

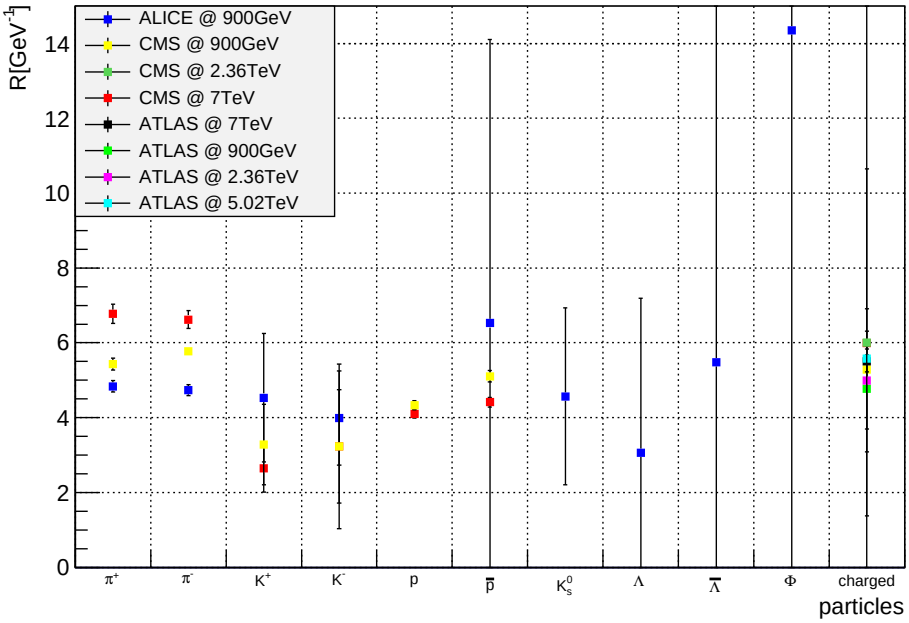

Figure 4.11: Calculated fireball radii for several particle spectra obtained from ALICE, CMS and ATLAS experiments at varying energies (Proton radius does not appear in graphic as including would have compromised the scaling).

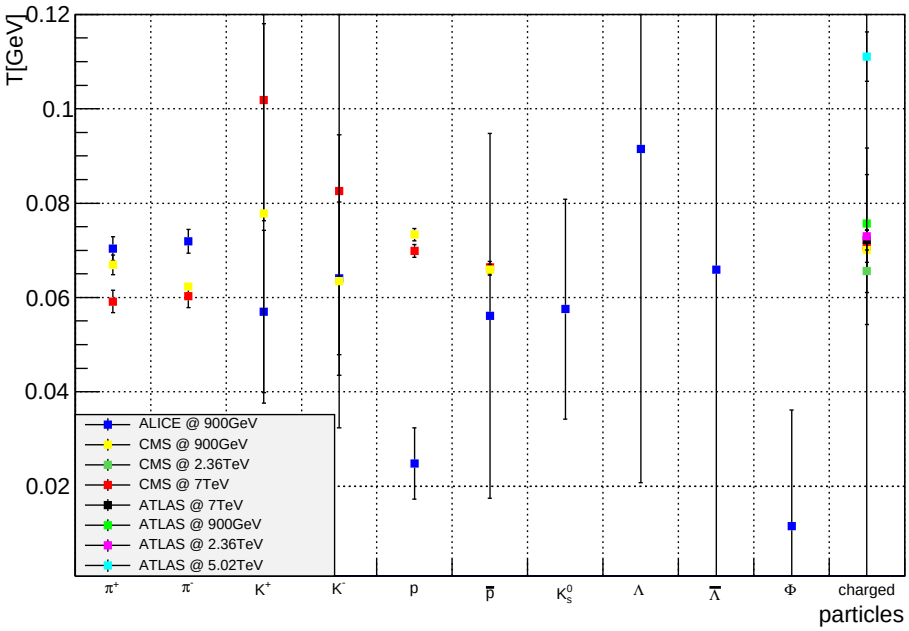

Figure 4.12: Calculated fireball temperatures for several particle spectra obtained from ALICE, CMS and ATLAS experiments at varying energies.

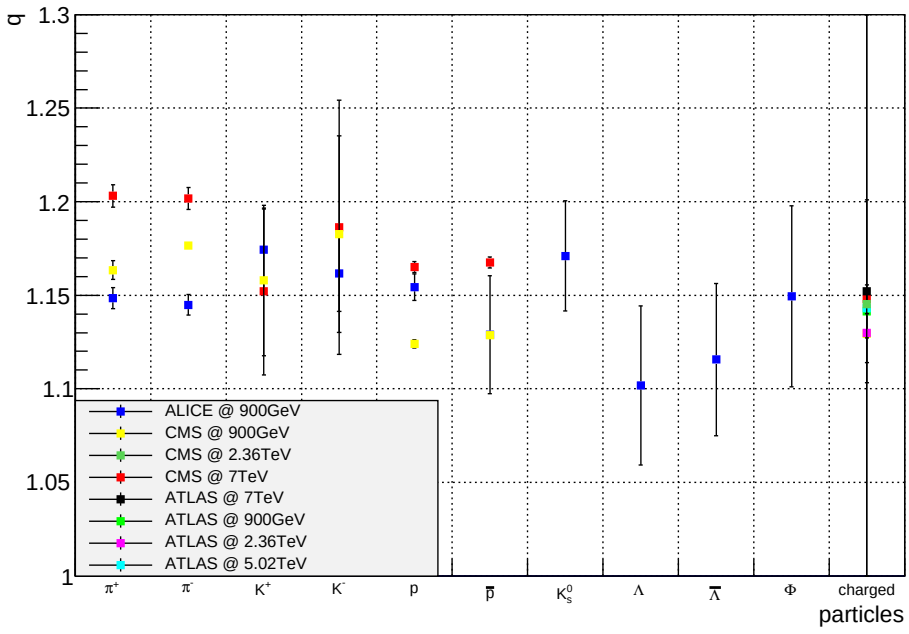

Figure 4.13: Calculated fireball q values for several particle spectra obtained from ALICE, CMS and ATLAS experiments at varying energies.

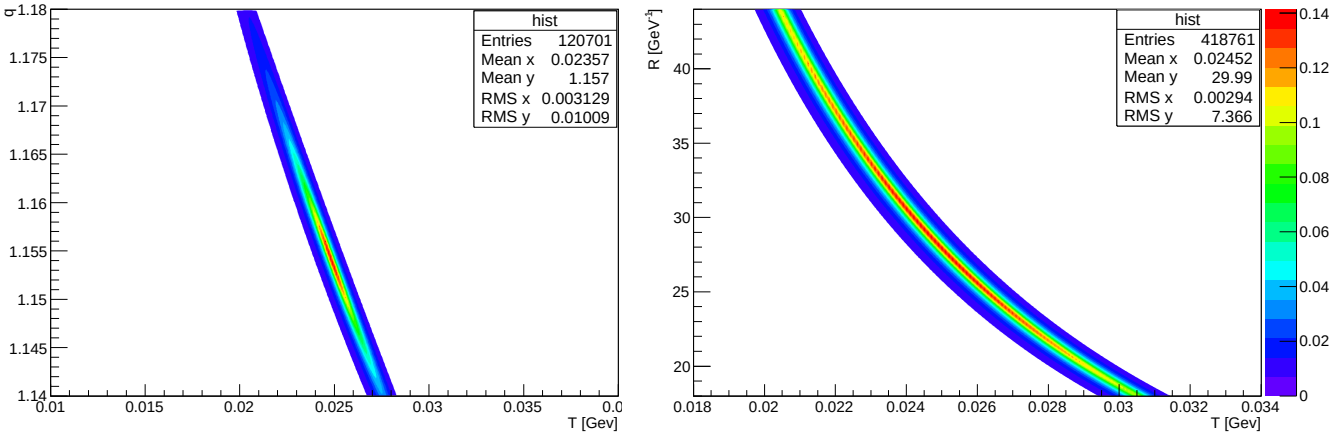

Figure 4.14: Contour plots of the multinormal probability density, for ALICE pp collision at 900 GeV, for proton. Left panel shows inverted χ^2 values as a function of (T, q) with R fixed at $R = 28\,\mathrm{GeV}^{-1}$. Right panel shows inverted χ^2 values as a function of (T, R) with q fixed at $q = 1.1543$.

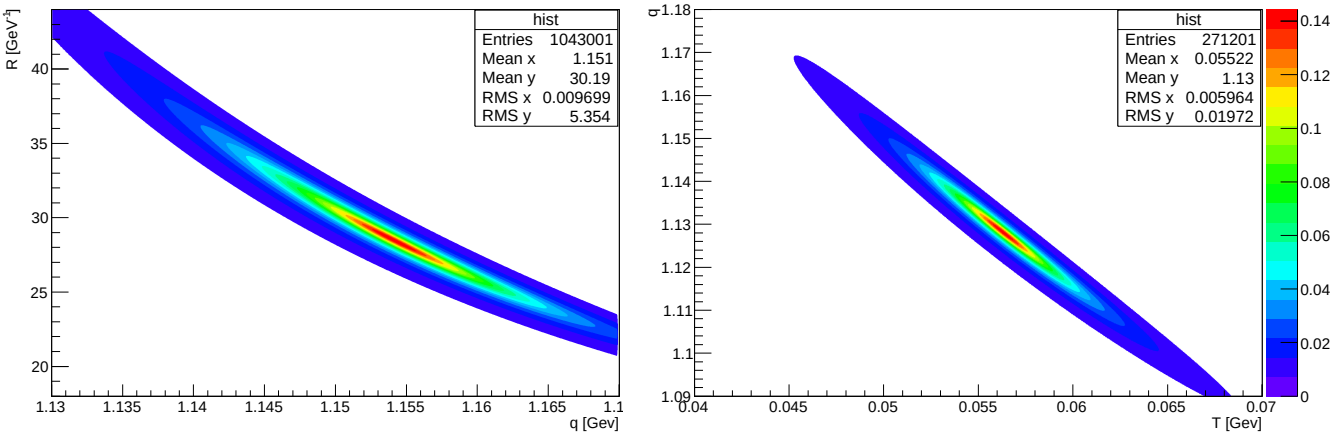

Figure 4.15: Contour plots of the multinormal probability density, for ALICE pp collision at 900 GeV, for proton (left panel) and antiproton (right panel) . Left panel shows inverted χ^2 values as a function of (q, R) with T fixed at $T = 0.056\,\text{GeV}$. Right panel shows inverted χ^2 values as a function of (q, T) with R fixed at $R = 6.5\,\text{GeV}^{-1}$.

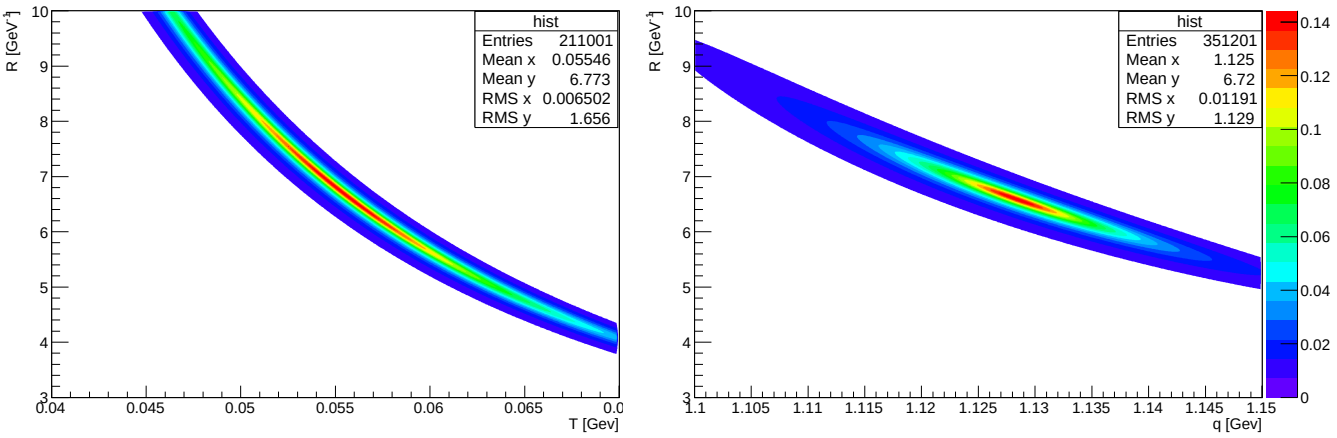

Figure 4.16: Contour plots of the multinormal probability density, for ALICE pp collision at 900 GeV, for antiproton. Left panel shows inverted χ^2 values as a function of (T, R) with q fixed at $q = 1.129$. Right panel shows inverted χ^2 values as a function of (q, R) with T fixed at $T = 0.056\,\text{GeV}$.

Chapter 5

Discussion

Fitting spectral data from pp collisions utilising a generalised statistical model, may seem like a questionable practice. The number of particles that typically emerge from such collisions are of the order of 30 or so particles. The premise for employing the methods of statistical physics in the analysis of a given physical system, is that the observed system is homogeneous and large enough such that the macroscopic properties of the system are not affected by microscopic fluctuations. With systems of the aforementioned size, we most certainly cannot claim this to be the case. However, it should be noted that in practice there are a number of systems which appear far from large in the statistical sense that still behave "statistically". Thus, when deciding to fit this data using the Tsallis model essentially we are testing the extent to which our model is valid, for it may still hold in these regimes. Statistical analyses of p-p data are mentioned in [28]. It is apparent from fig(4.2)-fig(4.6) that the fits using the Tsallis distribution described in (4.6) fit the data significantly better than the fits obtained using the BG distribution in (4.8). However, in the case of combined particle spectra (and particularly for the p-Pb collision), although qualitatively the fits appear good, quantitatively the χ^2/NDF values for these spectra are especially poor. These cases require further investigation. Unfortunately, it has been somewhat more difficult to establish the universality of the fit parameters with beam energy, $\sqrt{s}$. One can see this in fig(4.11)-fig(4.13). Not all the various parameter values have overlapping uncertainties. This may lead one to believe that perhaps there is

no universality of the parameters q, T and R, and thus no manner of establishing a relationship between these parameters and the beam energy, $\sqrt{s}$, such that parameter values at higher energies can be predicted. However, from a quantitative statistical analysis a more detailed analysis of the χ^2 distributions is required. In fact, it is noted in [29] that the q and T parameters are not independent but are strongly correlated. In fact they are linearly related. A linear relationship between q and T is mentioned in [30] and [31]. In [30] and [31] a Tsallis distribution is derived via considering a thermodynamic system, in contact with a heat bath, comprised of smaller subsystems (or clusters) with varying temperatures, T around some value T_0. If one then assumes a simple diffusion picture for the equalization of this temperature, the solution to the stochastic equation describing the evolution of T is given by a gamma distribution, namely:

$$g(1/T) = \frac{1}{\Gamma\left(\frac{1}{q-1}\right)} \frac{T_0}{q-1} \left(\frac{1}{q-1}\frac{T_0}{T}\right)^{\frac{2-q}{q-1}} \exp\left(-\frac{1}{q-1}\frac{T_0}{T}\right). \tag{5.1}$$

Convoluting (5.1) with the BG factor, $\exp(-E/T)$, they obtained a Tsallis distribution[1],

$$h_q = \frac{2-q}{T}\left[1-(1-q)\frac{E}{T}\right]^{\frac{1}{1-q}}, \tag{5.2}$$

describing the single particle distribution function. They went on to find that given the diffusion picture they could relate T and q via the following relation:

$$T = T_0 + (q-1)T_v, \tag{5.3}$$

where T_v and T_0 are a parameter described in [30]. Furthermore, under different considerations to [30] and [31] a linear relationship between T and q is also predicted in [32], in which solutions to the Boltzmann equation are considered in which the familiar two-particle energy composition rule, $E_{12} = E_1 + E_2$, is generalised to $E_{12} = h(E_1 E_2)$.

[1] the prefactor of $(2-q)/T$ is obtained via the normalization constraint $\int dE h_q(E) = 1$

In the case of $h(E_1, E_2) = E_1 + E_2$ the familiar Boltzmann distribution function is recovered, i.e.:

$$f(E) = f(0)e^{-\frac{E}{T}}; \tag{5.4}$$

however, in the case of the nonextensive energy composition rule, $h(E_1, E_2) = E_1 + E_2 + aE_1E_2$, where a is an energy scale related to the microscopical dynamics, a Tsallis distribution of the form:

$$f(E) = f(0)(1 + aE)^{-\frac{1}{aT}}. \tag{5.5}$$

Of course if one identifies $a = \frac{q-1}{T}$ a familiar Tsallis distribution is recovered. Although the Tsallis distributions obtained in [31] and [32] were derived under different considerations and are not of exactly the same form as ours, this linear relationship derived between T and q is worth mentioning. As mentioned in [29], the correlation between R and q is reflected in the elliptical (inverse) χ^2 squared distributions (at fixed R) in the left panel of fig(4.14) and the right panel of fig(4.15). As one traverses the semi-major axes of these ellipses the (inverse) χ^2 values do not change appreciably, and thus comparatively good fits are still attainable, even when some distance from the minimum. It is evident from table(4.2) that the correlation coefficients of T and q for all the measured hadrons display an extremely strong negative correlation (all the coefficients are very near -1, except for the ϕ meson, for which only a few data points were available for the fitting of the ϕ spectra). This suggests some negative linear causal relationship between the two parameters and in fact this inverse linear relationship can be seen when comparing fig(4.12) with fig(4.13). From fig(4.9) it is clear that the proton and antiproton data points virtually overlap (although granted the scale is logarithmic) over the entire p_t range. Consequently, one would expect that the values for the parameters obtained for these two extremely similar spectra to be near identical. Surprisingly however, the values differ substantially, despite the similarity of the resultant χ^2/NDF values. Furthermore, in the case of the proton and antiproton it is apparent from the right panel of fig(4.14) and from the left panel of

fig(4.16) that for fixed q as one proceeds along the hyperbole-like curve one can traverse a great distance before the (inverse) χ^2 values alter significantly. Similarly, one observes, from the left panel of fig(4.15) and the right panel of fig(4.16), that, at fixed T, as one moves away from the minimum along the semi-major axis of the ellipse-like contour, the (inverse) χ^2 values do not change appreciably. Evidently, given such considerations, the practice of fitting these parameters to a set of data becomes an extremely delicate process, which, one would imagine, would be highly sensitive to the data being fitted. Changing some parameter significantly may not increase the χ^2 value significantly, whilst simultaneously changing another may notably reduce it. The glaring disparity between the parameter values for the proton and antiproton, despite the noticeable similarities between their corresponding data sets, is indicative of such arguments. In fact, when we fixed the q value for the proton to that of the antiproton, i.e. $q = 1.12892$, it was observed that $T = 0.0553 \pm 0.0044\,\mathrm{GeV}$ and $R = 6.8 \pm 1.2\,\mathrm{GeV}^{-1}$. These values highly resemble those of the antiproton. It is apparent from fig(4.7) that the Tsallis distribution with this new set of parameters still provides a remarkably satisfactory fit to the data. Moreover the χ^2/NDF for the case of fixed q versus varying q are highly similar ($\sim 4\%$ difference). Therefore, given these considerations, it is possible that there are in fact universal values for the parameters q, T, and R which provide comparatively good fits for all the data sets - and in [33] relations for T, and q with $\sqrt{s}$ are described; however, due to the strong correlations of all the parameters and the extremely gradual variation of χ^2 values along certain paths of the aforementioned contour plots, obtaining these global values becomes a difficult practice. It should also be noted that in [34] several invariant spectra are fitted over a much larger p_t range ($\sim$ 100GeV) than those displayed in the previous section using a Tsallis distribution. Given that the Tsallis fits to these p_t spectra are so good this has the suggests that for single particle spectra there are only essentially 3 degrees of freedom needed to describe these distributions [34]. Consequently, although a hadronizing system formed in the process of particle production is exceptionally complex, very few degrees of freedom are relevant.

We have shown that the proposed Tsallis entropy, with the appropriate con-

straints, results in a generalised statistics that is thermodynamically consistent. Under the assumption that the four laws of thermodynamics hold true for all systems regardless of the microscopic mechanisms characteristic of said systems, it is imperative that our proposed entropy should generate relations that are thermodynamically consistent. Such success does indeed warrant this entropy being further considered. Perhaps what still requires further investigation is the physical origin of the q parameter measuring the nonextensivity of the system. This perhaps has not been addressed in a satisfactory manner but some explanations as to the physical significance of q have been made. In [31], a kind of physical significance is given to the parameter q. In this analysis, q is essentially a measure of this non-homogeneity of the fireball. More precisely, $q = 1 + \omega$, where ω is the relative fluctuation of the inverse temperature T between the subsystems of the fireball, i.e.:

$$\omega = \frac{\left\langle \left(\frac{1}{T}\right)^2 \right\rangle - \left\langle \frac{1}{T} \right\rangle^2}{\left\langle \frac{1}{T} \right\rangle^2}. \tag{5.6}$$

Evidently, given the definition of ω in (5.6), q is essentially a measure of the fluctuations of the temperatures in the cluster from the Boltzmann temperature T_0.

Chapter 6

Conclusion

In conclusion we have formulated a generalized nonextensive Tsallis entropy and statistics which in the limit $q \to 1$ the familiar SG entropy and BG statistics is recovered. Furthermore, the generalisation has the attractive property of being thermodynamically consistent, and thusly does not violate the four thermodynamic laws deemed characteristic of all systems. This nonextensive Tsallis entropy results in a much better fit to p_t spectra than the associated BG entropy. The Tsallis entropy gives extremely good fits to the single-species particle spectra of various hadrons. It does however, appear to fall somewhat short when considering combined particle spectra, and this should be further considered. In fact, given that Tsallis distributions appear to fit p_t spectra up to extremely high energies, [34], it may be concluded that the hadronization process obeys some generalised statistical process in which there are only three essential degrees of freedom.

Although a universal set of parameters could not be obtained, the prospect of acquiring such global fits for these parameters still appears to be a possibility. Furthermore, should these values be obtained, the behaviour of the parameters with respect to $\sqrt{s}$ can then be established. Deducing the relationship between the parameter values and $\sqrt{s}$ will provide a further means to test the plausibility of a generalised thermodynamical analysis in the evaluation of p_t spectra, contrary to the more common approach, which attributes the power-tail of p_t spectra to the dynamics within the system.

Within this framework there is still the question of the physical significance of the parameter q. Evidently, one would expect q to depend on the microscopic mechanisms of the system, however a rigorous approach in which a generalised entropy is derived under such considerations is yet to be established. Although there is extensive research on the topic, there is still much room for further investigation and development of Tsallis distributions and their applicability in high energy physics.

Appendix A

Boltzmann Statistics

$$S = -\sum p \ln p \tag{A.1}$$

Using quantum statistics the expression for the entropy is given by:

$$S = -\prod_{\nu}\sum_{n_\nu} \frac{e^{-\beta(\epsilon_\nu-\mu)n_\nu}}{\prod_\alpha z_\alpha} \ln\left(\frac{e^{-\beta(\epsilon_\nu-\mu)n_\nu}}{\prod_\gamma z_\gamma}\right) \tag{A.2}$$

Simplifying the expression in (A.2) we obtain the following:

$$\begin{aligned} S &= -\prod_{\nu} \frac{\sum_{n_\nu} e^{-\beta(\epsilon_\nu-\mu)n_\nu}}{\prod_\alpha z_\alpha} \left[-\beta(\epsilon_\nu-\mu)n_\nu - \ln\left(\prod_\gamma z_\gamma\right)\right] \\ &= \prod_{\nu}\sum_{n_\nu} \frac{\beta(\epsilon_\nu-\mu)n_\nu e^{-\beta(\epsilon_\nu-\mu)n_\nu}}{\prod_\alpha z_\alpha} + \prod_{\nu}\sum_{n_\nu} \frac{\ln\left(\prod_\gamma z_\gamma\right) e^{-\beta(\epsilon_\nu-\mu)n_\nu}}{\prod_\alpha z_\alpha} \\ &= \prod_{\nu}\sum_{n_\nu} \frac{\beta(\epsilon_\nu-\mu)n_\nu e^{-\beta(\epsilon_\nu-\mu)n_\nu}}{\prod_\alpha z_\alpha} + \ln\left(\prod_\gamma z_\gamma\right) \end{aligned} \tag{A.3}$$

But the first term in (A.3) can be expressed as a partial derivative, namely:

$$T\frac{\partial \ln\left(\prod_\nu z_\nu\right)}{\partial T} = \prod_{\nu}\sum_{n_\nu} \frac{\beta(\epsilon_\nu-\mu)n_\nu e^{-\beta(\epsilon_\nu-\mu)n_\nu}}{\prod_\alpha z_\alpha} \tag{A.4}$$

As such using (A.4) we can rewrite (A.3) as the following:

$$\begin{aligned} S &= T\frac{\partial \ln\left(\prod_\nu z_\nu\right)}{\partial T} + \ln\left(\prod_\gamma z_\gamma\right) \\ &= \frac{\partial}{\partial T} T \ln\left(\prod_\nu z_\nu\right) \\ &= \frac{\partial}{\partial T}\left(T \ln Z_{GC}\right) \end{aligned} \tag{A.5}$$

We know that for fermions and bosons $Z_{GC}^{FD,BE} = \prod_\nu \left(1 \pm e^{-\beta(\epsilon_\nu - \mu)}\right)^{\pm 1}$, therefore:

$$\ln Z_{GC}^{FD,BE} = \pm \sum_\nu \ln\left(1 \pm e^{-\beta(\epsilon_\nu - \mu)}\right). \tag{A.6}$$

Thus the entropy is given by:

$$S_{GC}^{FD,BE} = \sum_\nu \left\{ \ln\left(1 \pm e^{-\beta(\epsilon_\nu-\mu)}\right)^{\pm 1} + \beta(\epsilon_\nu - \mu)\left(\frac{e^{-\beta(\epsilon_\nu-\mu)}}{1 \pm e^{-\beta(\epsilon_\nu-\mu)}}\right)\right\} \tag{A.7}$$

$$= \sum_\nu \left\{ \mp \ln\left(\frac{1}{1 \pm e^{-\beta(\epsilon_\nu-\mu)}}\right) + \left(\frac{\beta(\epsilon_\nu-\mu)}{e^{\beta(\epsilon_\nu-\mu)} \pm 1}\right)\right\} \tag{A.8}$$

$$= \sum_\nu \left\{ \mp \left[\ln\left(\frac{e^{\beta(\epsilon_\nu-\mu)}}{e^{\beta(\epsilon_\nu-\mu)} \pm 1}\right)\right] + \left(\frac{\beta(\epsilon_\nu-\mu)}{e^{\beta(\epsilon_\nu-\mu)} \pm 1}\right)\right\} \tag{A.9}$$

$$\begin{aligned} &= \sum_\nu \left\{ \mp \left[\left(\frac{e^{\beta(\epsilon_\nu-\mu)} \pm 1}{e^{\beta(\epsilon_\nu-\mu)} \pm 1}\right) \ln\left(\frac{e^{\beta(\epsilon_\nu-\mu)}}{e^{\beta(\epsilon_\nu-\mu)} \pm 1}\right)\right]\right. \\ &\left. + \left(\frac{\beta(\epsilon_\nu-\mu)}{e^{\beta(\epsilon_\nu-\mu)} \pm 1}\right)\right\} \end{aligned} \tag{A.10}$$

$$= \sum_{\nu} \left\{ \mp \left[\pm \frac{1}{e^{\beta(\epsilon_\nu - \mu)} \pm 1} \ln \left(\frac{e^{\beta(\epsilon_\nu - \mu)}}{e^{\beta(\epsilon_\nu - \mu)} \pm 1} \right) \right. \right.$$
$$\left. \left. + \frac{e^{\beta(\epsilon_\nu - \mu)}}{e^{\beta(\epsilon_\nu - \mu)} \pm 1} \ln \left(\frac{e^{\beta(\epsilon_\nu - \mu)}}{e^{\beta(\epsilon_\nu - \mu)} \pm 1} \right) \right] + \left(\frac{\beta(\epsilon_\nu - \mu)}{e^{\beta(\epsilon_\nu - \mu)} \pm 1} \right) \right\} \tag{A.11}$$
$$= \sum_{\nu} \left\{ \mp \left[\pm \frac{1}{e^{\beta(\epsilon_\nu - \mu)} \pm 1} \ln \left(\frac{1}{1 \pm e^{\beta(\epsilon_\nu - \mu)}} \right) \right. \right.$$
$$\left. \left. \pm \frac{\beta(\epsilon_\nu - \mu)}{e^{\beta(\epsilon_\nu - \mu)} \pm 1} + \frac{e^{\beta(\epsilon_\nu - \mu)}}{e^{\beta(\epsilon_\nu - \mu)} \pm 1} \ln \left(\frac{e^{\beta(\epsilon_\nu - \mu)}}{e^{\beta(\epsilon_\nu - \mu)} \pm 1} \right) \right] + \left(\frac{\beta(\epsilon_\nu - \mu)}{e^{\beta(\epsilon_\nu - \mu)} \pm 1} \right) \right\} \tag{A.12}$$
$$= \sum_{\nu} \left\{ - \frac{1}{e^{\beta(\epsilon_\nu - \mu)} \pm 1} \ln \left(\frac{1}{1 \pm e^{\beta(\epsilon_\nu - \mu)}} \right) \right.$$
$$\left. - \frac{\beta(\epsilon_\nu - \mu)}{e^{\beta(\epsilon_\nu - \mu)} \pm 1} \mp \frac{e^{\beta(\epsilon_\nu - \mu)}}{e^{\beta(\epsilon_\nu - \mu)} \pm 1} \ln \left(\frac{e^{\beta(\epsilon_\nu - \mu)}}{e^{\beta(\epsilon_\nu - \mu)} \pm 1} \right) + \left(\frac{\beta(\epsilon_\nu - \mu)}{e^{\beta(\epsilon_\nu - \mu)} \pm 1} \right) \right\} \tag{A.13}$$
$$= - \sum_{\nu} \left\{ n_\nu \ln n_\nu \pm (1 \mp n_\nu) \ln(1 \mp n_\nu) \right\} \tag{A.14}$$

Appendix B

Kinematics

This is a brief summary of the several kinematic quantities that are employed in relativistic high energy physics and are often used in the main text of this work. Further information can be found in [35]. It should be noted that natural units are used throughout the text such that $c = \hbar = k \equiv 1$, unless otherwise stated.

B.1 Rapidity and pseudorapidity

Usually the 4-momentum of an object is written as $p^\mu = (p_0, p_x, p_y, p_z)$ where $p_0 = E$ and p_x, p_y, p_z are the x, y and z components of the 3-momentum respectively, but often in high energy physics it is more convenient to write the 4-momentum in the form $p^\mu = (p_0, \vec{p_t}, p_z)$. This is because boosts are often taken to be along the z-axis and as such this is seperated from the transverse momentum, $\vec{p_t}$, along the xy-axis. A quantity that is often used in high energy physics is the rapidity. The rapidity is defined as:

$$y \equiv \frac{1}{2} \ln \left(\frac{p_0 + p_z}{p_0 - p_z} \right) \tag{B.1}$$

We can take the exponential of $-y$ and $+y$ in (B.1) to get:

$$\begin{aligned} e^y + e^{-y} &= \sqrt{\frac{p_0 + p_z}{p_0 - p_z}} + \sqrt{\frac{p_0 - p_z}{p_0 + p_z}} \\ &= \sqrt{\frac{(p_0 + p_z)^2}{p_0^2 - p_z^2}} + \sqrt{\frac{(p_0 - p_z)^2}{p_0^2 - p_z^2}} \end{aligned} \tag{B.2}$$

but $p_0^2 - p_z^2 = m^2 + p_t^2$. If we define the transverse mass to be $m_t^2 \equiv m^2 + p_t^2$, then (B.2) becomes:

$$\begin{aligned} e^y + e^{-y} &= \frac{p_0 + p_z}{m_t} + \frac{p_0 - p_z}{m_t} \\ e^y + e^{-y} &= \frac{2p_0}{m_t} \\ E &= m_t \cosh y \end{aligned} \tag{B.3}$$

In a similar manner it can be shown that $p_z = m_t \sinh y$.

Another quantity that is often used is the pseudorapidity defined to be:

$$\eta \equiv \frac{1}{2} \ln \left(\frac{|\vec{p}| + p_0}{|\vec{p}| - p_0} \right) \tag{B.4}$$

When $|\vec{p}| >> m$ it is clear that $\eta \to y$. In high energy physics experiments this is usually the case. If we take the angle θ to be the polar angle to the beam axis (given to be along the z-axis) then the pseudorapidity can be written in a more instructive

form:

$$\begin{aligned}\eta &= \frac{1}{2}\ln\left(\frac{|\vec{p}|+|\vec{p}|\cos\theta}{|\vec{p}|-|\vec{p}|\cos\theta}\right)\\ &= \ln\left(\sqrt{\frac{1+\cos\theta}{1-\cos\theta}}\right)\\ &= \ln\left(\frac{\sin\theta}{1-\cos\theta}\right)\\ &= \ln\left(\frac{2\sin(\frac{\theta}{2})\cos(\frac{\theta}{2})}{2\sin^2(\frac{\theta}{2})}\right)\\ &= -\ln\left[\tan\left(\frac{\theta}{2}\right)\right] \end{aligned} \tag{B.5}$$

B.2 Pressure in a non-interacting gas

Pressure is given by $P = F/A$, but the force is given by:

$$F = \frac{\Delta p}{\Delta t} \tag{B.6}$$

Looking at an ideal gas, if we let n_{right} denote the average number of particles per unit volume moving to the right, we may ask the question how many of these particles are colliding into a wall with area A in some time Δt. This is given by

$$n = n_{right} A v \Delta t \tag{B.7}$$

Where v represents one the magnitude of the volicity of one of this particles moving to the right (Obviously this is not correct as each particle moving to the right will be doing so with a unique velocity). Thus the average time taken between each collision is given by:

$$\Delta t = \frac{1}{n_{right} A v_x} \tag{B.8}$$

Of course the momentum transfer in this process will be $\Delta p = 2p_x$, and as such the the pressure of the gas will be given by:

$$P = 2p_x n_{right} v_x \tag{B.9}$$

but the number of particles moving to the right will be half those moving both left and right as such, let n be the number of particles moving in either direction along the x-axis as such:

$$P = p_x n v_x \tag{B.10}$$

Furthermore, in non-relativistic mechanics $v_x = p_x/m$ and as such the pressure is given by:

$$P = \frac{p_x^2 n}{m} \tag{B.11}$$

We since the particle clearly have different momenta we average the p_x^2 values. Furthermore there should be no difference between the x, y and z directions and as such $\bar{p_x^2} = \bar{p_y^2} = \bar{p_z^2}$. But $\bar{p^2} = \bar{p_x^2} + \bar{p_y^2} + \bar{p_z^2} = 3\bar{p_x^2}$. As such our expression for the pressure is given by:

$$P = \frac{\bar{p^2} n}{3m} \tag{B.12}$$

For the case of relativistic mechanics we recognize that $p_x = \gamma m_0 v_x$, and so the expression for the pressure is given by:

$$\begin{aligned} P &= \frac{\bar{p^2} n}{3\gamma m_0} \\ &= \frac{\bar{p^2} c^2 n}{3\gamma m_0 c^2} \\ &= \frac{\bar{p^2} c^2 n}{3E} \end{aligned} \tag{B.13}$$

In natural units this is given by:

$$P = \frac{\bar{p^2} n}{3E} \tag{B.14}$$

Bibliography

[1] J. Cleymans and D. Worku, Eur. Phys. J. A **48**, 160 (2012).

[2] Particle Data Group, K. Nakamura *et al.*, J. Phys. **G37**, 075021 (2010).

[3] M. Stephanov, J.Phys. **G38**, 124147 (2011).

[4] A. Andronic, P. Braun-Munzinger, and J. Stachel, Nuclear Physics A **772**, 167 (2006).

[5] M. Gell-Mann, Physics Letters **8**, 214 (2014).

[6] G. Zweig, CERN-TH412 (1964).

[7] D. Griffiths, *Introduction to elementary particles* (John Wiley & Sons, 2008).

[8] J. C. Collins, D. E. Soper, and G. F. Sterman, Adv.Ser.Direct.High Energy Phys. **5**, 1 (1988), hep-ph/0409313.

[9] J. Collins and M. Perry, Phys. Rev. Lett. **34**, 1353 (1975).

[10] F. Karsch, Nucl.Phys. **A698**, 199 (2002), hep-ph/0103314.

[11] D. H. Rischke, Prog.Part.Nucl.Phys. **52**, 197 (2004), nucl-th/0305030.

[12] K. Redlich, Journal of Physics: Conference Series **5**, 162 (2005).

[13] R. Pathria, *Statistical mechanics* (Butterworth Heinemann, Oxford, UK, 1996).

[14] E. Jaynes, Phys. Rev. **106**, 620 (1957).

[15] R. Mendes, A. Plastino, and C. Tsallis, Physica A **261**, 534 (1998).

[16] C. Tsallis, Eur. Phys. J. A **13**, 371 (2002).

[17] Z. Włodarczyk and G. Wilk, Phys. Rev. Lett. **84**, 2770 (2000).

[18] F. Cooper and G. Frye, Phys. Rev. D **10**, 186 (1974).

[19] C. Tsallis, J. Stat **52**, 479 (1988).

[20] F. Büyükiliç, D. Demirhan, and A. Güleç, Physics Letters A **197**, 209 (1995).

[21] T. Biró, Z. Schram, and K. Ürmössy, Journal of Physics G: Nuclear and Particle Physics **37**, 094027 (2010).

[22] J. Conroy, H. Miller, and A. Plastino, Phys.Lett. **A374**, 4581 (2010), 1006.3963.

[23] M. Rybczyński and Z. Włodarczyk, Eur.Phys.J. **C74**, 2785 (2014), 1401.5639.

[24] STAR Collaboration, B. Abelev *et al.*, Phys.Rev. **C75**, 064901 (2007), nucl-ex/0607033.

[25] PHENIX Collaboration, A. Adare *et al.*, Phys.Rev. **C83**, 064903 (2011), 1102.0753.

[26] ALICE Collaboration, K. Aamodt *et al.*, Eur.Phys.J. **C71**, 1655 (2011), 1101.4110.

[27] CMS Collaboration, V. Khachatryan *et al.*, Phys.Rev.Lett. **105**, 022002 (2010), 1005.3299.

[28] J. Cleymans and K. Redlich, Phys.Rev.Lett. **81**, 5284 (1998), nucl-th/9808030.

[29] I. Sena and A. Deppman, Eur.Phys.J. **A49**, 17 (2013), 1209.2367.

[30] Z. Włodarczyk and G. Wilk, Eur.Phys.J. **A48**, 161 (2012), 1203.4452.

[31] Z. Włodarczyk and G. Wilk, Eur. Phys. J. A **40**, 299 (2009).

[32] T. Biro and G. Purcsel, Phys.Rev.Lett. **95**, 162302 (2005), hep-ph/0503204.

[33] K. Urmossy, arXiv preprint arXiv:1212.0260 (2012).

[34] G. Wilk and C.-Y. Wong, Acta Physica Polonica B **43** (2012).

[35] C. Y. Wong, *Introduction to high-energy heavy-ion collisions* (World scientific, 1994).

[36] C. Beck and E. G. D. Cohen, Physica A **322**, 267 (2003).

[37] J. Cleymans, G. Hamar, P. Levai, and S. Wheaton, J. Phys. G: Nucl. Part. Phys. **36**, 064018 (2009), 0812.1471.

[38] J. Cleymans and K. Redlich, p. 1 (2008), 9903063v2.

[39] T. Biró, Z. Schram, and K. Ürmössy, Journal of Physics G: Nuclear and Particle Physics **37**, 094027 (2010).